2016

Investigating The Effects of Glutathione and Other Key Proteins on Iron Homeostasis and Subcellular Redox Balance in Yeast Model Systems

Kirsten Renee Collins
University of South Carolina

Investigating The Effects of Glutathione and Other Key Proteins on Iron Homeostasis and Subcellular Redox Balance in Yeast Model Systems

By

Kirsten Renee Collins

Bachelor of Science

Western Carolina University, 2012

Submitted in Partial Fulfillment of the Requirements

For the Degree of Master of Science in

Chemistry

College of Arts and Sciences

University of South Carolina

2016

Accepted by:

Caryn E. Outten, Director of Thesis

F. Wayne Outten, Reader

Cheryl L. Addy, Vice Provost and Dean of the Graduate School

Dedication

I would like to dedicate this thesis to my late grandmother, Edith Collins. You were always proud of me for continuing my education and your generous gifts helped to make graduate school a possibility for me. I know the last few years of your life were difficult and I couldn't visit you as often as I wanted but you still made me feel loved every time I saw you. And even though you won't see me receive my degree, I know that you would be proud.

Acknowledgements

First and foremost, I would like to thank Dr. Caryn Outten for being a great advisor and giving me support even through difficult times. I would like to thank all of the past and present Outten lab members that stuck with me through the day-to-day grind of graduate school; especially Dr. Angela Albetel, Dr. Adrienne Dlouhy, Dr. Max Darch, and John Hepburn for teaching me so much and keeping things lighthearted, Malini Gupta for all of the great talks, Evan Talib for making us all laugh, Hatice Ozer, Crystal McGee, Dr. Vidyadhar Daithankar, Tirthankar Bandyopadhyay, and all of the Wayne Outten lab members for all of your help through the years. I would also like to specially thank Caroline Schlee for keeping me positive and making lab more bearable.

I especially would like to thank Adrienne, my parents and the rest of my family for supporting me and all of my crazy ideas throughout the years and being proud of me, no matter where I end up.

I owe my greatest thanks to my future husband, Stefan, for supporting me through the worst times and celebrating with me during the best times. I wouldn't be the same person without you.

Abstract

Iron homeostasis in *Saccharomyces cerevisiae* is controlled through several pathways and is important because too much iron can cause cellular damage. Iron homeostasis in yeast is primarily controlled by transcription factors Aft1 and Aft2 which bind to the iron regulon to induce iron uptake when iron levels are low. When iron levels are sufficient, Aft1 and Aft2 are bound and inhibited by monothiol glutaredoxins (Grxs) Grx3 and Grx4. These Grxs are also involved in iron trafficking in the cell and bind to and deliver iron-sulfur clusters to multiple proteins.

The first part of this thesis focuses on determining if excess GSH/GSSG disrupts iron trafficking in *grx3 grx4* mutant strains (*grx3*Δ*grx4*Δ) and (*grx3*Δ Gal-*GRX4*). Total and oxidized glutathione were increased in Δ*grx3*Δ*grx4* compared to wild type (WT). Total and oxidized glutathione was higher in Δ*grx3* Gal-*GRX4* than WT 40 hours after galactose removal, but by 64 hours a suppressor mutation developed and glutathione levels resembled those of WT. Δ*grx4* Gal-*GRX3* had the same issue. The increased glutathione previously observed in literature were not able to be replicated. Experiments of expression levels of *GSH1* were inconclusive.

The second part of this thesis looks at iron homeostasis in budding yeast *Saccharomyces cerevisiae* and fission yeast *Schizosaccharomyces pombe*. These species utilize homologous proteins as well as proteins unique to each species. In *S. pombe*,

glutaredoxin, Grx4, interacts with and regulates the iron-dependent transcriptional repressor Php4. Similar to its homologues, Grx4 forms a [2Fe-2S]-bridged homodimer alone, and a [2Fe-2S]-bridged heterocomplex when co-expressed with Php4. When iron is sufficient, Grx4 interacts with Php4 to form a [2Fe-2S] cluster-bound complex, communicating cellular iron status and inhibiting Php4 activity. Fra2 was often insoluble and unstable. Coexpressing Fra2 with Pphp4 or Grx4 did not improve the stability. A urea extraction of Fra2 expressed independently improved solubility but Fra2 was still unstable. Fra2 coexpressed with the Takara chaperones did not improve the solubility.

The third portion of this thesis involves glutathione reducing reactive oxygen species (ROS) and maintaining redox balance within the cell. A rxYFP sensor was targeted to the mitochondrial intermembrane space (IMS) in order to measure the redox status of this subcellular compartment when the cell was exposed to oxidative stress. The hope for this work is to answer questions about the redox states and mechanisms controlling redox homeostasis on the subcellular level. The rxYFP sensor in the HGT1 overexpression strain as well as in the empty vector control was much more reduced than previously observed. Troubleshooting experiments were unable to resolve this issue.

Table of Contents

List of Figures

Chapter 1

Introduction

Iron Homeostasis in *Saccharomyces cerevisiae*

Iron is an important cofactor in electron transfer and is important for all life. Iron is involved in many processes within the cell such as DNA replication, nitrogen fixation (Zimmermann and Hurrell, 2007), the tricarboxylic acid cycle and respiration (Jacques et. al., 2014). Iron is critical for every type of cell, but too much iron, or too little, can lead to health issues. In humans, too little iron can lead to anemia, while too much iron can catalyze formation of hydroxyl radicals (Jacques et. al., 2014) and lead to iron overload diseases such as hemochromatosis. Yeast are eukaryotic cells that are often used as model systems for human systems, and thus are also sensitive to the changing levels of iron. Luckily, there are systems in place to regulate iron within the cells.

In *Saccharomyces cerevisiae* iron homeostasis is controlled by a few key proteins (Figure 1.1). When iron levels are high, transcriptional activator Yap5 binds DNA to express genes of the Yap5 regulon which includes iron-sequestering protein Tyw1 (Li et. al., 2011) and vacuolar iron transporter Ccc1 among others (Li et. al., 2008). Transcription factors Aft1 and Aft2 are deployed when iron levels in the cell are low. They accumulate in the nucleus and bind DNA at the iron regulon. The iron regulon is turned on, iron uptake genes are expressed, and iron is transported into the cell from extracellular sources and intracellular storage (Outten and Albetel, 2013). When iron levels are sufficient,

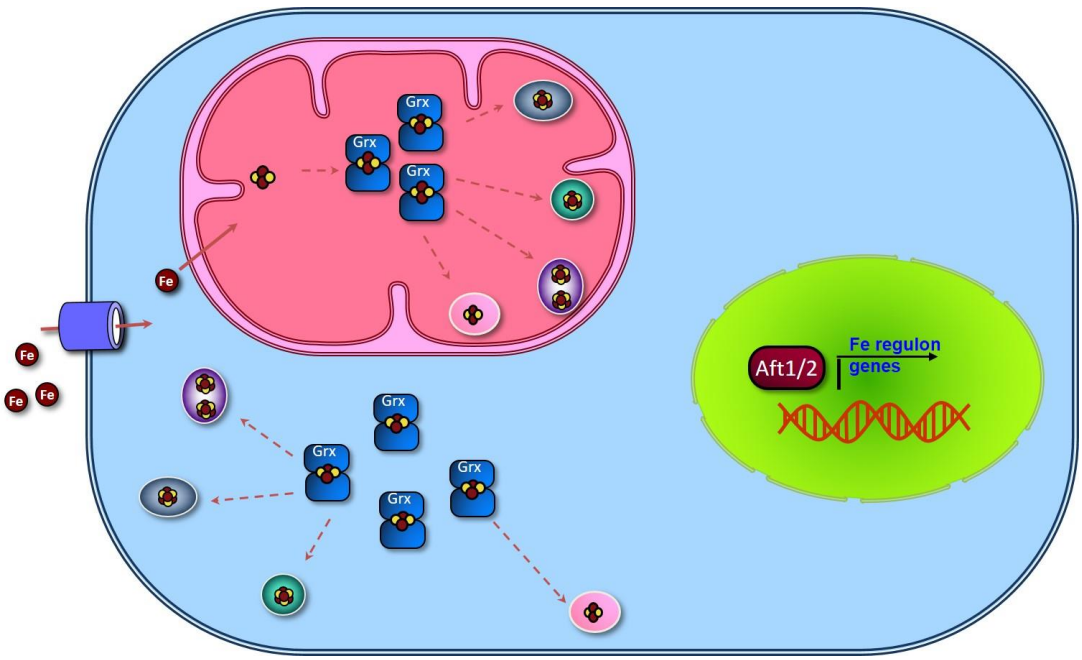

Figure 1.1 Key proteins involved in iron homeostasis of *S. cerevisiae*. Glutaredoxins (Grx) along with Fra2 move into the nucleus and transfer an Fe-S cluster to Aft1/2 and turn off iron regulon genes under iron sufficiency conditions. Adapted from C. Outten (unpublished).

glutaredoxins 3 (Grx3) and 4 (Grx4) form a complex along with an iron-sulfur cluster and cytosolic proteins Fra1 and Fra2. This cluster inhibits Aft1/2 which are sequestered to the cytosol by nuclear the exportin Msn5 (Poor et. al., 2014) (Outten and Albetel, 2013). These glutaredoxin proteins are also involved in iron homeostasis of *Schizosaccharomyces pombe*.

Iron homeostasis in *Schizosaccharomyces pombe*

Iron homeostasis in the fission yeast *Schizosaccharomyces pombe* utilizes different proteins than in *S. cerevisiae* (Figure 1.2). When iron levels are high, the GATA-type transcription factor, Fep1, binds DNA and represses the expression of genes involved in iron uptake. If iron levels drop too low, Php4 along with Php2, Php3, and Php5 down-regulates genes involved in iron-utilizing proteins, iron-requiring metabolic pathways and iron-sulfur cluster biogenesis machinery (Mercier et. al., 2006) (Mercier et. al., 2008). Monothiol glutaredoxins are present in *S. pombe* iron homeostasis as well. As in *S. cerevisiae*, glutaredoxins transport iron in the form of iron-sulfur clusters as well as sense cellular iron levels. Grx4 inhibits Fep1 DNA binding in low iron conditions to stop the inactivation of iron uptake genes. As for high iron conditions, Grx4 is proposed to form a homodimer containing an iron-sulfur cluster that no longer allows Grx4 to interact with Fep1 (Jacques et. al., 2014). Grx4 also interacts with Php4 in an iron-dependent manner and disrupts Php4 from binding DNA which stops the inactivation of iron-utilization genes (Jacques et. al., 2014). BolA-like protein Fra2 is involved in *S. pombe* iron homeostasis similarly to its involvement in *S. cerevisiae*. Fra2 is a binding partner to Fep1 and is

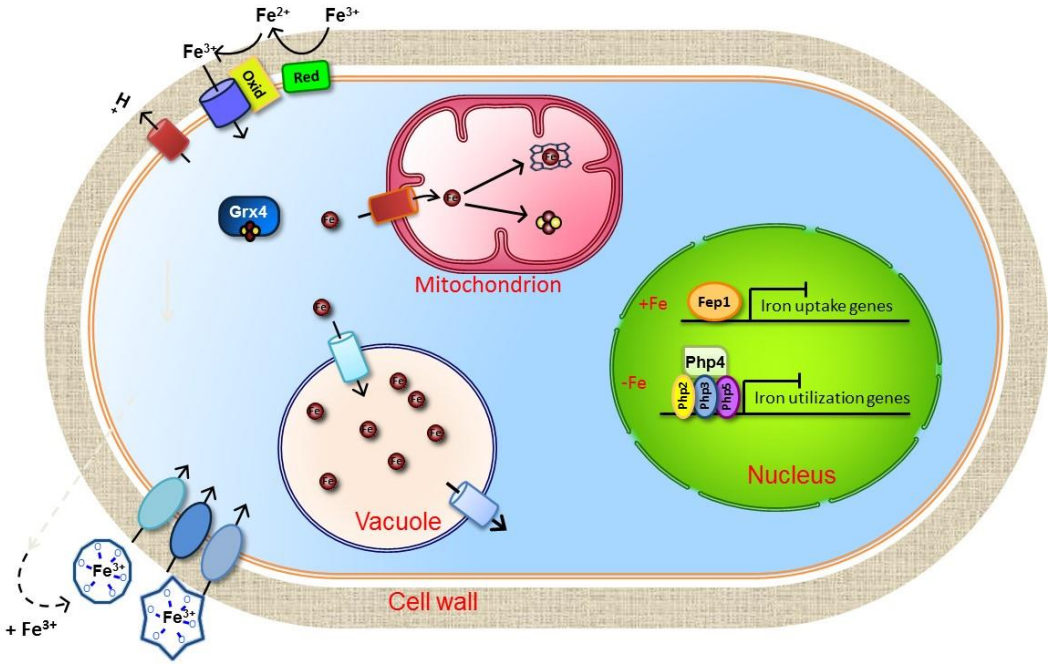

Figure 1.2 Key proteins involved in iron homeostasis of *S. pombe*. Transcription factor Fep1 binds DNA under low iron conditions to turn on iron uptake genes. Php4, along with Php2/3/5 bind DNA during high iron conditions to turn on iron utilization genes. Adapted from (Outten 2013).

required to complete the inactivation process of Fep1 binding by Grx4 (Jacques et. al., 2014).

Role of glutathione in iron homeostasis and cellular redox

Monothiol glutaredoxins are heavily involved in iron transport, sensing, and homeostasis. All monothiol glutaredoxins are classified by their conserved CGFS active site which binds iron-sulfur clusters. Glutaredoxins (Grxs) form $[2Fe\text{-}2S]^{2+}$-bridged homodimers by utilizing cysteines from both Grxs and two molecules of reduced glutathione (GSH) (Li and Outten, 2012). Glutathione is a small tripeptide that serves many functions in the cell. Glutathione not only participates in iron signaling and iron-sulfur biogenesis (Muhlenhoff, et al., 2010), it also performs proofreading functions, removes reactive oxygen species and xenobiotics, and reduces oxidative stress through thiol redox control (Baudouin-Cornu et. al., 2012). Glutathione is synthesized in two steps by γ-glutamylcysteine synthetase and glutathione synthetase (Baudouin-Cornu et. al., 2012). Another aspect of GSH homeostasis is degradation of GSH to glutamate, glycine and cysteine, which is completed by the Dug complex including subunits Dug1, Dug2, and Dug3. Two of the three subunits, Dug2 and Dug3, are primarily responsible for GSH degradation since *dug1* deletion only partially impairs GSH degradation (Baudouin-Cornu et. al., 2012). In yeast, GSH enters the cell by way of plasma membrane transporter, Hgt1, and GSH can be stored in the vacuole by transporter Ycf1 (Figure 1.3) (Baudouin-Cornu et. al., 2012). Glutathione can undergo reversible oxidation (Figure 1.4). The reduced for (GSH) can react with reactive oxygen species to convert to the oxidized form (GSSG).

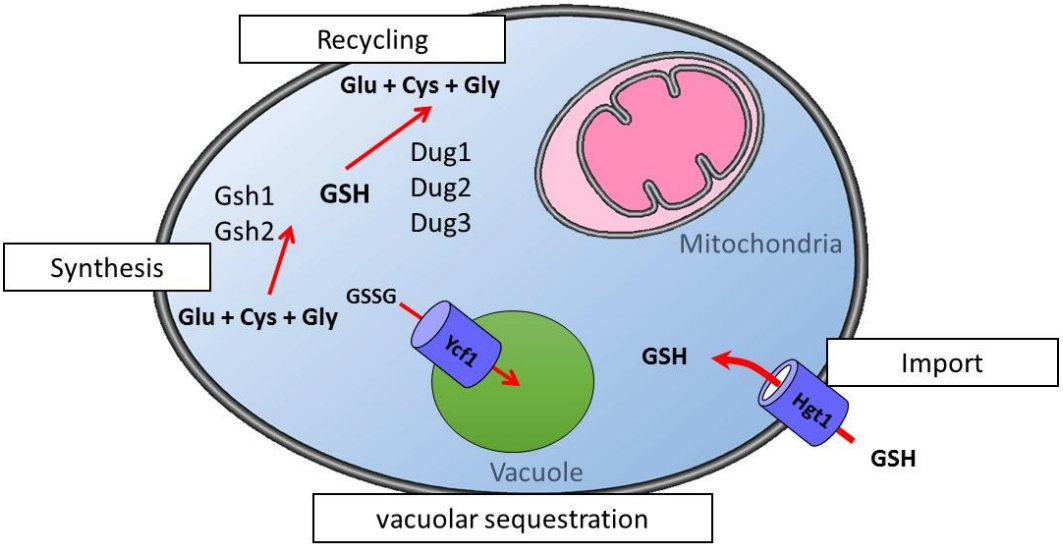

Figure 1.3 Glutathione homeostasis in *S. cerevisiae*. Glutathione is synthesized by Gsh1/2, and recycled by the Dug proteins. Extracellular glutathione can be imported through Hgt1 and within the cell, glutathione can be stored in the vacuole by vacuolar importer Ycf1.

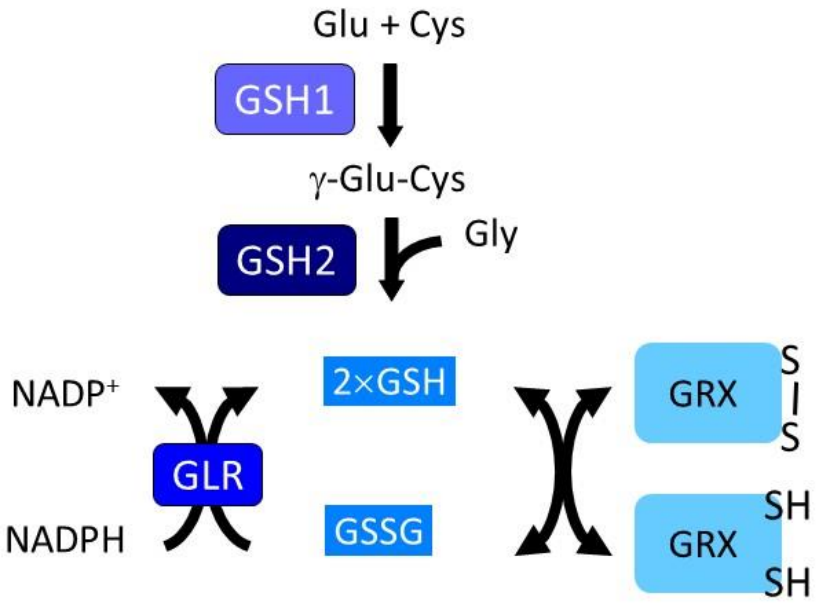

Figure 1.4 Reversible oxidation of glutathione. Glutathione is synthesized by Gsh1/2.Oxidized glutathione can be reduced by glutathione reductase (GLR) using NADPH as a cofactor. Adapted from C. Outten.

GSSG is converted back to GSH by glutathione reductase (GLR) which makes glutathione a major component of cellular redox control. (Kolossov, et al., 2014).

Scope of thesis

This thesis outlines the interactions of iron homeostasis and glutathione redox control in yeast models *Saccharomyces cerevisiae* and *Schizosaccharomyces pombe*. The effects of excess glutathione in *S. cerevisiae* lacking Grx3 and Grx4 will be covered in chapter 2. The in vitro study of the interaction of Php4 and Grx4 with cofactor Fra2 in *S. pombe* will be covered in chapter 3. The redox potentials of the mitochondrial intermembrane space when exposed to high levels of glutathione will be covered in chapter 4. Additional details of the methods described in the above chapters will be provided in chapter 5. Overall, this work looks at multiple key players in yeast iron homeostasis.

Chapter 2

Understanding the effects of excess glutathione on iron trafficking in *Saccharomyces cerevisiae*

Abstract

Iron homeostasis in *Saccharomyces cerevisiae* is controlled through several pathways and is important because too much iron can cause cellular damage. Iron homeostasis in yeast is primarily controlled by transcription factors Aft1 and Aft2 which bind to the iron regulon to induce iron uptake when iron levels are low. When iron levels are sufficient, Aft1 and Aft2 are bound and inhibited by monothiol glutaredoxins (Grxs) Grx3 and Grx4. These Grxs are also involved in iron trafficking in the cell and bind to and deliver iron-sulfur clusters to multiple proteins. Previous studies that examined the iron-trafficking by Grx3 and Grx4 used double deletion strains that lack both *GRX3* and *GRX4* genes (*grx3*Δ*grx4*Δ) or a single *grx3*Δ deletion strain with *GRX4* under the control of a galactose-inducible promoter (*grx3*Δ Gal-*GRX4*) allowing galactose-dependent control of *GRX4* expression. Interestingly, the galactose-inducible strain exhibits a dramatic increase in glutathione (GSH) levels upon *GRX4* repression. High reduced (GSH) and oxidized (GSSG) glutathione levels have been shown to disrupt iron homeostasis as well. The goal of this work is to determine if it is the increased levels of GSH/GSSG, rather than the deletion of Grx3 and Grx4, which disrupts the iron trafficking in these strains. Total and

oxidized glutathione, measured by the Promega Glo Assay or enzyme cycling assay, were increased in Δ*grx3*Δ*grx4* compared to wild type (WT). Total and oxidized glutathione was higher in Δ*grx3* Gal-*GRX4* than WT 40 hours after galactose removal, but by 64 hours a suppressor mutation developed and glutathione levels resembled those of WT. Δ*grx4* Gal-*GRX3* had the same issue. The increased glutathione previously observed in literature were not able to be replicated. Experiments of expression levels of *GSH1* were inconclusive

Introduction

Iron homeostasis in the model eukaryote *Saccharomyces cerevisiae* involves many proteins in several pathways. The focus of this work is a few key players in this process. Yeast is used as a model system because it is a simple eukaryotic organism that it easy to grow and genetically manipulate. Despite its simplicity and ease of growth, many proteins in the yeast iron homeostasis pathway have mammalian homologs (Askwith and Kaplan, 1998). Thus, research on iron homeostasis in yeast has been able to answer questions not only about the processes and proteins found in yeast but has also been relevant to similar studies in mammalian cells. The importance of this project goes much further than just its relatability to human homologs, since there are many unknown components of the iron trafficking and sensing pathways in yeast.

When iron levels are low, iron import genes in the yeast iron regulon are activated by the binding of transcription factors Aft1 and Aft2. Aft1/2-regulated genes in the iron regulon includes genes for cell surface iron uptake, such as *FET3* and *FIT3*, as well as genes that code for siderophore uptake and iron transport across the vacuole membrane.

When the cell has sufficient iron, these transcription factors are localized in the cytosol by the binding of monothiol Grxs Grx3 and Grx4 and the iron regulon is inhibited (Outten and Albetel, 2013). Monothiol Grxs have multiple roles in iron homeostasis and are found across several species including humans. Unlike most of the Grx family, monothiol Grxs lack oxidoreductase activity. They all have conserved structures: a thioredoxin domain at the N-terminus and one or two monothiol Grx domains at the C-terminus with conserved cysteine residues used in Fe-S cluster binding (Pujol-Carrion and de la Torre-Ruiz, 2010). These Grxs have homologous proteins spanning multiple species across domains. Grxs, in addition to binding Aft1/Aft2, also help assemble and transport iron sulfur (Fe-S) clusters to target proteins. Grx3 and Grx4 located in the cytosol bind a bridging [2Fe-2S] cluster using the active site cysteine of the Grx domain and glutathione (GSH) as ligands and participate in iron signaling within the cell (Outten and Albetel, 2013).

GSH is a tripeptide of glutamate, cysteine, and glycine that participates in thiol-disulfide exchange reactions and as a cofactor for enzymes that detoxify reactive oxygen species and xenobiotics (Baudouin-Cornu et. al., 2012). GSH also helps with proofreading of protein folding and takes part in iron signaling and Fe-S cluster biosynthesis. GSH homeostasis within the cell is dependent upon several pathways. The first is GSH synthesis which occurs in two steps catalyzed by gamma-glutamylcysteine synthase and glutathione synthase, which are expressed by the *GSH1* and *GSH2* genes, respectively (Toledano et.al., 2013). The oxidized form of GSH, glutathione disulfide (GSSG), is recycled back to its reduced form by glutathione reductase (Iwema, et al., 2009) (Bandyopadhyay et.al., 2008). GSH is also imported into the cell by the plasma membrane oligopeptide transporter Hgt1 (Toledano et. al., 2013). Another aspect of GSH homeostasis is degradation of GSH to

glutamate, glycine and cysteine, which is completed by the Dug complex including subunits Dug1, Dug2, and Dug3. Two of the three subunits, Dug2 and Dug3, are primarily responsible for GSH degradation since *dug1* deletion only partially impairs GSH degradation (Baudouin-Cornu et. al., 2012). Excess GSH in the cell can be transported into the vacuole by Ycf1 (Baudouin-Cornu et. al., 2012). These processes together keep GSH levels stable.

A previous study looked at the role of Grx3 and Grx4 in iron trafficking and sensing in the cells (Muhlenhoff, et al., 2010). *S. cerevisiae* strains lacking Grx3 and Grx4 were utilized with two different mutants: a double knockout, *grx3*Δ*grx4*Δ, and a galactose-regulated mutant, *grx3*Δ Gal-*GRX4* (Muhlenhoff, et al., 2010). Iron-trafficking by the *grx3*Δ Gal-*GRX4* mutant strain was tested by measuring the enzymatic activity of iron-containing enzymes. It was found that the activity was severely reduced when Grx3 and Grx4 were not present suggesting that Grx3/4 were involved with iron-trafficking (Muhlenhoff, et al., 2010). An additional experiment measured GSH and GSSG in both mutant strains and found that the *grx3*Δ Gal-*GRX4* had accumulated GSH (Muhlenhoff, et al., 2010). It is unexplained why *grx3*Δ Gal-*GRX4* has accumulation of GSH when *grx3*Δ*grx4*Δ does not. However, high levels of GSH itself can disrupt iron homeostasis as shown by an experiment that measured iron import at varying levels of GSH and found increased GSH can cause iron import genes to be induced (Muhlenhoff, et al., 2010) (Kumar, et al., 2011) (Ojeda, et al., 2006). Thus, elevated GSH can disrupt iron homeostasis and trigger an iron-starvation-like response within the cell. It was proposed that the excess GSH could be inactivating cytosolic Fe-S cluster-containing enzymes which in turn impacts iron regulation since Aft2 (and presumably Aft1) are Fe-S cluster binding

proteins (Kumar, et al., 2011) (Poor, et al., 2014). The main goal of this project is to determine whether the decreased activity of the iron containing enzymes, resulting from iron trafficking anomalies, in *grx3*Δ Gal-*GRX4* is caused by the lack of Grx3/Grx4 or is affected due to high levels of GSH that accumulate in the strain.

Materials and Methods

Yeast Strains, and Media The *S. cerevisiae* strains used in this study are wild type strains BY4742 **(***MATα his3Δ1 leu2Δ0 lys2Δ0 ura3Δ0*) and W303-1A (*MATa ura3-1 ade2-1 trp1-1 his3-11,15 leu2-3,112*) both from Roland Lill and BY4742 (*MATα his3Δ1 leu2Δ0 ura3Δ0*) from Andy Dancis. Mutants used in this study are *grx3*Δ*grx4*Δ (BY4742 *grx3::LEU2; grx4::KanMX4*) from Roland Lill, *grx3*Δ Gal-*GRX4* (W303-1A *pGRX4::GAL-L-natNT; grx3::LEU2*) from Roland Lill, and *grx4*Δ Gal-*GRX3* (BY4742 Δ*grx4::KanMX His3MX6-pGAL1-3HA-GRX3*) obtained from Andrew Dancis. Yeast strains were grown in synthetic complete (SC) media supplemented with 2% glucose, 2% galactose or 2% raffinose as the carbon source and all appropriate amino acids.

Growth Conditions All growth was started on synthetically defined (SD) media with all amino acids, 50μM $FeCl_3$ and 2% galactose. Strains were grown 2 to 3 days on plates from freezer stocks (Kirsten's box) at 30 °C. Cells were then moved to liquid SD media with 2% galactose and grown overnight. ODs were kept between 1-2. Cultures grown at 30 °C in shaking incubator. After 24 hours, cells were collected, washed twice with 1 mL sterile water and resuspended in media containing 2% glucose. Cells were harvested 40 and 64 hours after removing galactose according to the Glo assay protocol.

The growth process had to be altered several times to attempt to find conditions that minimized development of secondary suppressor mutations in *grx3*Δ Gal-*GRX4* these changes are described in more detail below. Bradford assays were used to quantify the protein concentrations in the samples.

GSH/GSSG Quantification using GSH/GSSG-Glo™ Assay The GSH content was quantified using the GSH/GSSG-Glo™ Assay, which utilizes the GSH present to convert a luciferin derivative to luciferin by way of a GSH S-transferase. This reaction is coupled to a firefly luciferase reaction which luminesces more intensely as more luciferin is formed. Extracts of these cultures were made by spinning down 1.8 x 10^6 cells at 10,000 rpm for 1.5 minutes then removing the supernatant (a sample of the supernatant in this step can be used to quantify extracellular GSH). Pellets were resuspended in 90 µL of 1X Passive lysis buffer and vortexed with 20 µL glass beads to lyse cells. Samples were centrifuged for 30 seconds at 5000 rpm and 20 µL aliquots were taken from the supernatant then used in the GSH/GSSG Glo™ Assay (Promega). The Synergy H1 Hybrid Reader (Biotech) was used to quantify GSH and GSSG levels. The protein concentration was quantified via the Bradford assay (Bio-Rad).

GSH/GSSG Quantification using DTNB Enzyme Cycling Assay GSH is a substrate used in the reaction that converts DTNB to TNB. TNB is yellow in color and the rate at which it forms can be directly related to the amount of GSH present. Whole cells are grown to mid-log and $2x10^7$ cells are centrifuged at 12,000 rpm for 10 seconds. Cells are resuspended in 50 µL ice-cold 1% sulfosalicylic acid (SSA). Cells are lysed with glass beads for 4 minutes then 200 µL 1% SSA is added and cells are incubated on ice for 30 min. Cells are centrifuged 5 minutes at 13,000 rpm then supernatant is transferred to a new

tube. Mitochondrial and PMS extracts can also be made by utilizing the pestle method with SM buffer (250 mM sucrose, 10 mM MOPS, pH 7.2) (see subcellular fractionation protocol below). GSSG measurements can be made by adding 1 µL 2-vinylpyridine, which binds reduced GSH, to 50 µL of the bead lysate or PMS extract. Then 1 µL 25% triethanolamine is added to bead lysate and PMS extracts and 0.5 µL 25% triethanolamine is added to mitochondria extracts. Then extracts are incubated for 60 minutes at room temperature. GSH/GSSG standards are prepared in 1% SSA. For the assay 20 µL of lysate or standard is added to a cuvette with 970 µL assay mixture (1 M Na-phosphate pH 7.5, 500 mM EDTA, 2 mM NADPH, 2 mM DTNB, 100 U/mL GSSG reductase, H_2O) and absorbance is measured at 412 nm at 15 second intervals for 2 minutes.

GSH1 western blot analysis Samples were grown to exponential phase and harvested at 3000 rpm for 5 minutes. Supernatant was removed and cells were washed with sterile water. 1:1 ratio of sample to glass beads was added and 1.67:1 ratio of lysis buffer. Cells were vortexed to lyse and centrifuged once for 5 minutes at 13,000 rpm followed by twice for 10 minutes at the same speed. Supernatant was transferred to a new tube after each step. 60 µg of sample was heated at 95 °C and loaded on a 12% tris-glycine gel. Transfer was performed then membrane was blocked in Odyssey blocking buffer overnight. Primary antibody, anti-Gsh1 (kind gift of J. Barycki) was added at 1:5000 ratio for 1 hour followed by anti-rabbit IgG (IRDye, LI-COR Lincoln, NE) at 1:25000 ratio for 1 hour.

Results and Discussion

Confirmation of accumulated GSH in Grx3/4 mutants Previous studies have shown that yeast strains lacking Grx3 and Grx4 have near-wild type levels of GSH, while *grx3*Δ Gal-*GRX4* showed 10-fold increase in GSH levels compared to wild type (Muhlenhoff, et al., 2010). To confirm these results, GSH and GSSG levels were first measured in the double deletion strain *grx3*Δ*grx4*Δ and the wild type control, BY4742 (Figure 2.1). The results indicate that both total and oxidized glutathione were higher in *grx3*Δ*grx4*Δ than the isogenic wild type control. The results obtained with *grx3*Δ*grx4*Δ differ from a previous report indicating that GSH and GSSG levels were not elevated in this double mutant (Muhlenhoff, et al., 2010). The reason for this discrepancy is not clear, but may stem from differences in the growth conditions used to assay the cells. The results suggest that GSH metabolism is disrupted through an unknown mechanism.

The previously cited paper also quantified GSH levels in *grx3*Δ Gal-*GRX4* and its wild type control strain, W303-1A. This trend was not verified (Figure 2.2), the Gal-*GRX4* *grx3*Δ strain has a 2-fold higher level of total glutathione than its wild type after 40 hours of growth in raffinose, however, by the 64 hour mark the levels were similar. The case was the same with the oxidized glutathione (5-fold increase) however, there was a large difference in total and oxidized glutathione levels. This result is most likely due to a suppressor mutation developing between 40 and 64 hours after galactose removal.

Growth optimization The growth rate of the *grx3*Δ Gal-*GRX4* strain suggested that a suppressor mutation occurred between 40 and 64 hours after galactose removal (Figure 2.3). This likely occurred due to high stress put on the cells in the absence of Grx3 and Grx4 and highlights the critical role played by these proteins. To reduce this potential

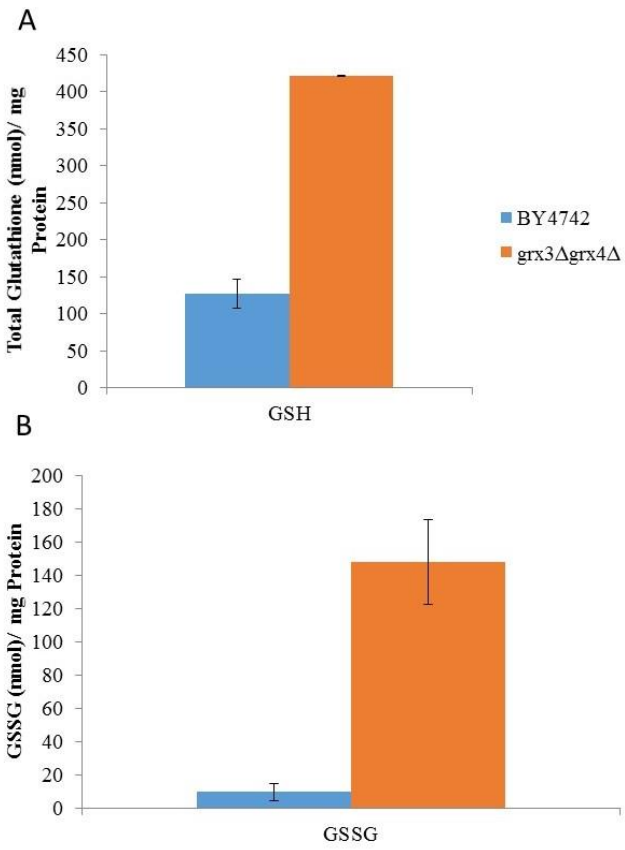

Figure 2.1. Total and oxidized glutathione in *grx3*Δ*grx4*Δ and wild type. Measured with Promega GSH/GSSG Glo after 24 hours of growth in SD media with 2% glucose. Measurements made in triplicate with standard deviations marked with error bars.

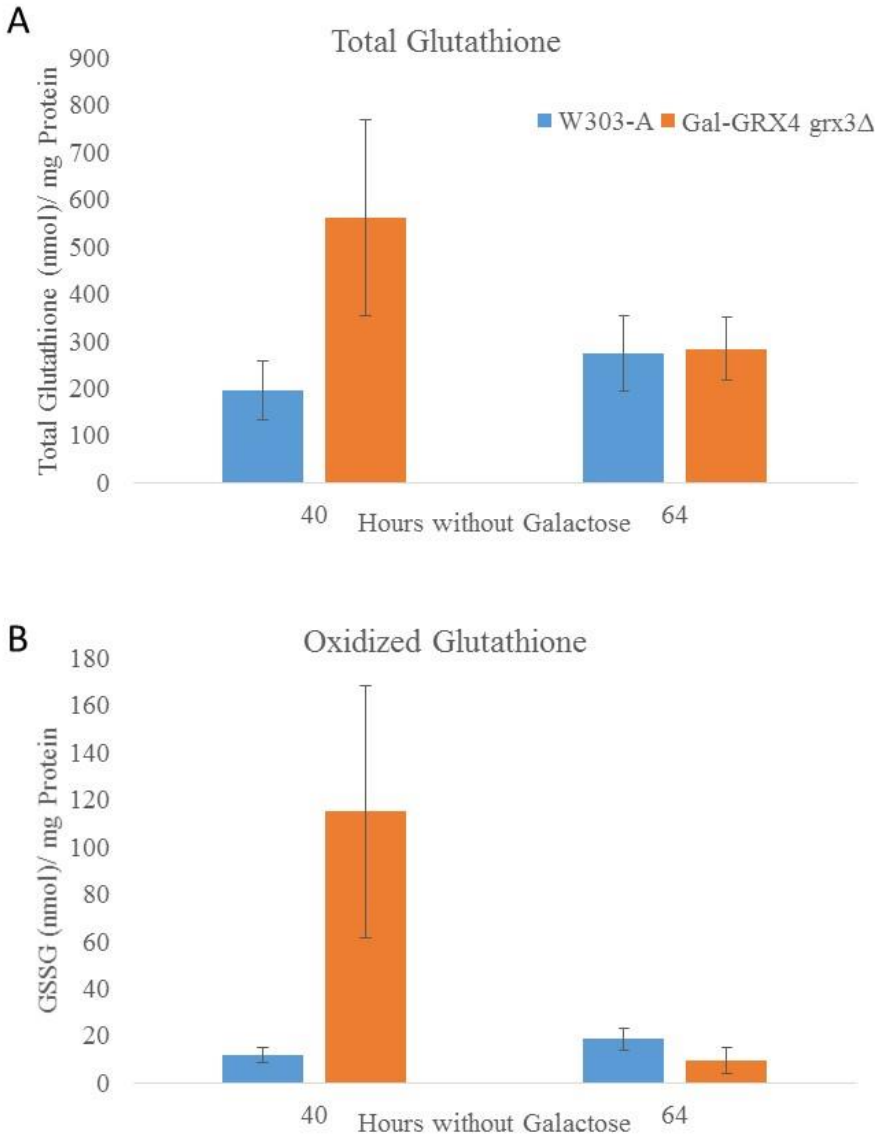

Figure 2.2. Total and oxidized glutathione in Gal-*GRX4 grx3*Δ and wild type. Total glutathione (A) and oxidized glutathione (B) measured with Promega GSH/GSSG Glo Assay at time points 40 hours and 64 hours after removal of galactose. Measurements made in triplicate with standard deviations marked with error bars.

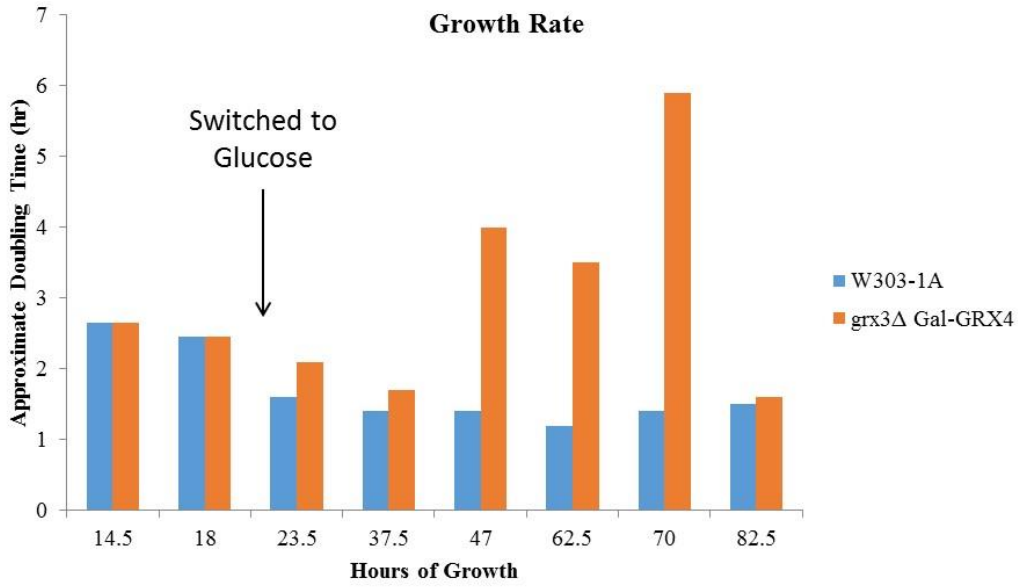

Figure 2.3. Approximate doubling time of *grx3*Δ Gal-*GRX4* compared to wild type. Measurements based on OD_{600} measurements. Galactose removed from media at indicated time.

stress, growth conditions were optimized. The following changes were made: culture ODs kept below 1, cells grown with and without iron chloride, cells were grown in a non-shaking incubator at 30°C to reduce oxidative stress, 2% raffinose was substituted for glucose, the wash step was removed so that the galactose was removed over time. No change was observed except for the removal of the wash step which allowed the suppressor mutations to occur at a later time. The measurements made at 40 and 64 hours were not reproducible because of mutations forming.

*Substituting grx4*Δ *Gal-GRX3* Suppressor mutations were observed in *grx3*Δ Gal-*GRX4* so *grx4*Δ Gal-*GRX3* strain was graciously provided by Dr. Andrew Dancis and was tested in the same way. Stocks of this strain were made in 1 mL SC 2% galactose and 250 µL 50% sterile glycerol and stored in Kirsten's box at -70 °C. The suppressor mutation also occurred in this strain around the same time (Figure 2.4). Overall, the results seen in the literature were not replicated in our lab. The general trend was similar, but the 10-fold increase of glutathione did not occur (Figure 2.5).

GSH1 expression To determine relative levels of glutathione synthesis, the expression of *GSH1* was characterized by western blot analysis (Figure 2.6). Samples were grown in galactose, then raffinose with no wash step and prepared according to the whole cell western procedure. (see chapter 5). Similar *GSH1* expression was observed in all samples, however, loading was uneven as shown by the control, *PGK1*. Experiment needs to be repeated under different growth conditions. Expression of *GRX3* in *grx4*Δ Gal-*GRX3* needs to be tested under multiple growth conditions.

In the future, the strains should be sequenced after mutating to characterize the mutation. Growth of strains could be extended so galactose is removed for 64 hours, then

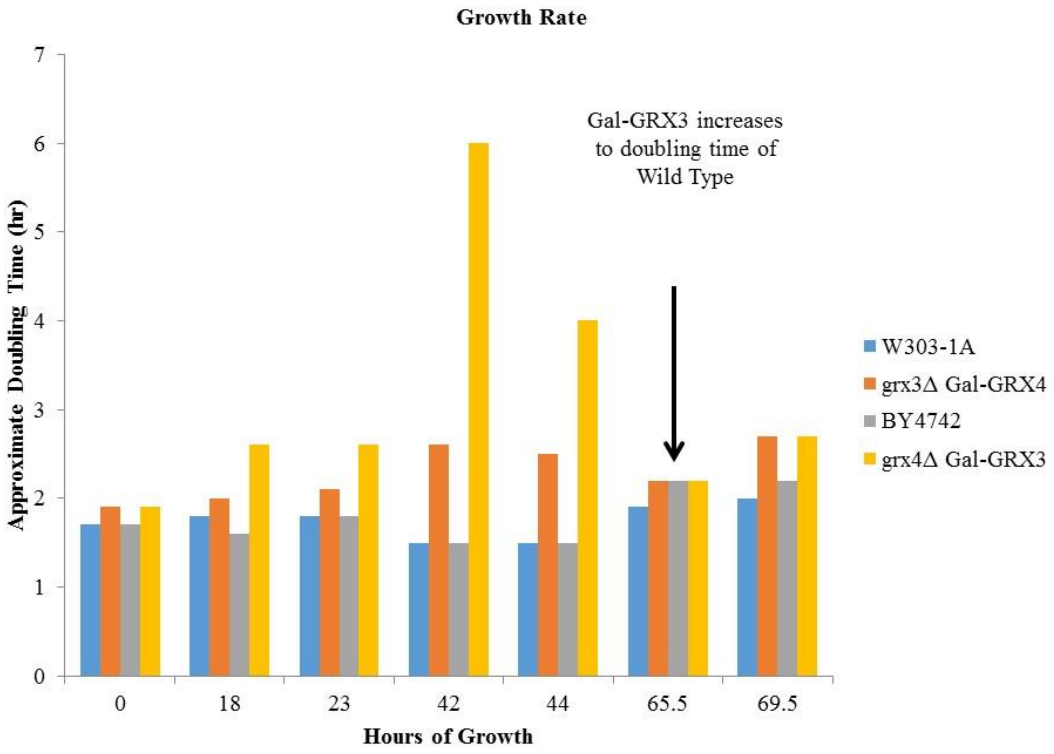

Figure 2.4 Growth rate of galactose regulated strains. Measurements based on OD_{600} measurements. Galactose removed from media at 23 hours.

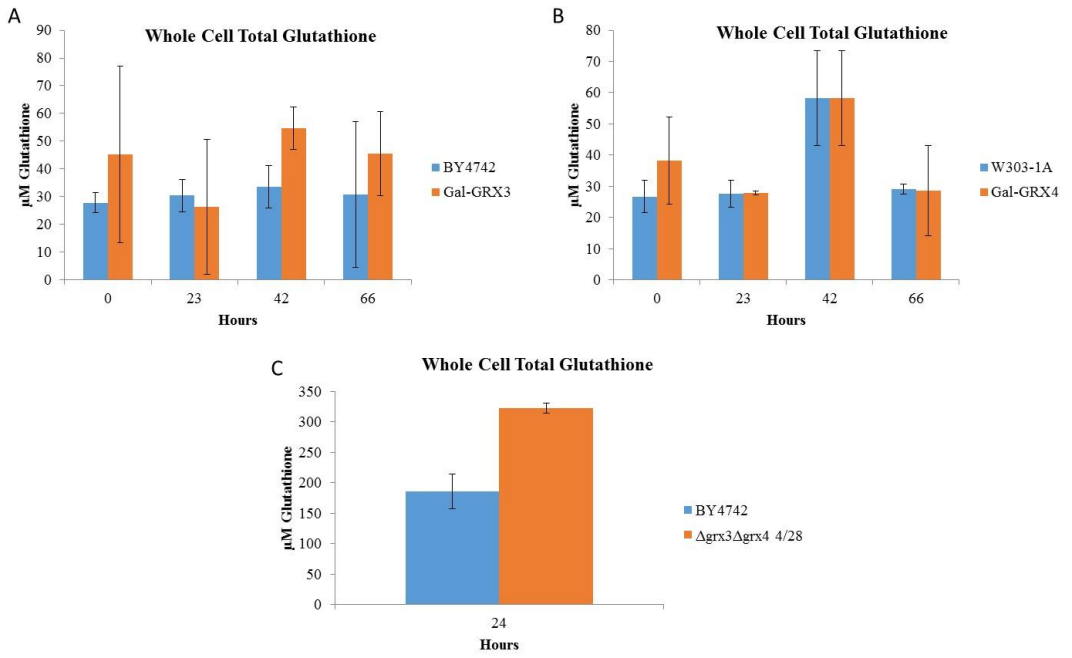

Figure 2.5 Total glutathione measurements. Total glutathione in Gal-*GRX3* Δ*grx4* (A), Gal-*GRX4* Δ*grx3* (B), and Δ*grx3*Δ*grx4* (C) strains with corresponding wild type strains measured with enzyme cycling assay at 23, 40, and 66 hours after removal of galactose. 50 mL cultures were grown in SD media containing 50 µM $FeCl_3$, 0.5% galactose and 2% raffinose at 30 °C in a shaking incubator. Throughout growth all cultures were diluted to remain below OD=2. Measurements made in triplicate with standard deviations marked with error bars.

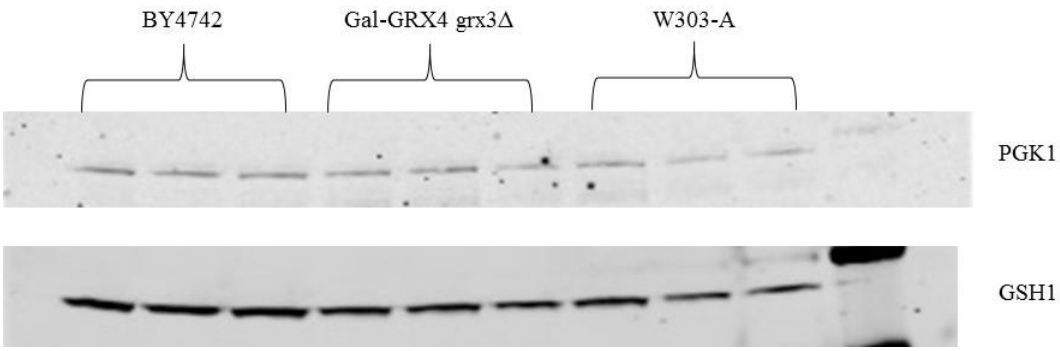

Figure 2.6 *GSH1* western blot of Gal-*GRX4* Δ*grx3* strain. *PGK1* (top) is a loading control. *GSH1* (bottom) antibody used to show relative Gsh1 expression. Samples were grown in SD 2% galactose then washed and moved to SD 2% raffinose. Extracts were taken after 24 hours of growth following galactose removal. Measurements are expected to have taken place before suppressor mutations formed. Each sample was grown and blotted in triplicate.

replaced for 24-64 hours, then removed once again determine if the same trends are seen. Also, more western blot analyses could be done to determine relative levels of *GRX3* and *GSH1* in the cultures during each stage of growth.

Chapter 3

Investigating the interaction of Fra2 with other key proteins involved in iron homeostasis of *Schizosaccharomyces pombe*

Abstract

Iron is required for a variety of intracellular metabolic pathways, yet increased intracellular iron is potentially damaging to cells. Organisms have developed multi-layered iron regulation pathways for maintaining sufficient levels of this essential cofactor. Iron homeostasis in budding yeast *Saccharomyces cerevisiae* and fission yeast *Schizosaccharomyces pombe* utilizes homologous proteins as well as proteins unique to each species. In *S. cerevisiae*, iron regulation is primarily controlled by the iron-responsive transcription factors Aft1 and Aft2 which can be inhibited by the monothiol glutaredoxins Grx3 and Grx4. In *S. pombe*, a homologous glutaredoxin, Grx4, interacts with and regulates the iron-dependent transcriptional repressor Php4. Similar to its homologues, Grx4 forms a [2Fe-2S]-bridged homodimer alone, and a [2Fe-2S]-bridged heterocomplex when co-expressed with Php4. When iron is sufficient, Grx4 interacts with Php4 to form a [2Fe-2S] cluster-bound complex, communicating cellular iron status and inhibiting Php4 activity. Fra2 was often insoluble and unstable. Coexpressing Fra2 with Pphp4 or Grx4 did not improve the stability. A urea extraction of Fra2 expressed independently improved

solubility but Fra2 was still unstable. Fra2 coexpressed with the Takara chaperones did not improve the solubility.

Introduction

Iron homeostasis in the fission yeast, *Schizosaccharomyces pombe*, involves some major differences than the processes in *Saccharomyces cerevisiae*. Cellular iron levels are controlled using two transcription factors, Fep1 and Php4 which reciprocally regulate each other's expression in an iron-dependent manner. When iron levels are high, Fep1 binds to DNA and represses the transcription of iron uptake genes (Pelletier B, 2002). Under low iron conditions, Php4 is localized to the nucleus where it is recruited to the CCAAT-binding complex, which is composed of Php2, Php3, and Php5. The CCAAT-binding complex allows Php4 to repress transcription for iron utilization genes to downshift iron-dependent processes such as mitochondrial respiration, amino acid and heme biosynthesis, iron sulfur cluster assembly, and the TCA cycle and conserve iron in the cell (Mercier et al, 2008). The localization of Php4 is controlled by both exportin Crm1 and monothiol glutaredoxin Grx4 (Mercier and Labbé, 2009). It has been found that Grx4 physically interacts with Php4 at the C-terminal and Php4 interacts with both the N-terminal and C-terminal regions of Grx4. (Vachon et al, 2012). This interaction is required to localize Php4 from the nucleus back to the cytosol when iron levels are no longer lacking. (Mercier et al, 2006; Mercier et al, 2008; Mercier and Labbé, 2009). Previous work in our lab was done to characterize the in vitro iron-dependent interaction between Grx4 and Php4 (Dlouhy, 2015).

Previous work in our lab found that Grx4 binds a cluster with and without Php4. Fra2 is able to displace one Grx4 monomer from Grx4 homodimer to form a Fra2-Grx4 heterodimer. It was expected that Php4 could have a similar interaction with Grx4. However, unlike the case with the Fra2-Grx3/4 interaction in *S. cerevisiae, S. pombe* Grx4 homodimer is not converted to a Php4-Grx4 complex upon titration with apo-Php4. In *S. cerevisiae*, Fra2 forms a complex with Grx3/4 and assists a cluster transfer to Af1/2 which then homodimerizes. It was thought that Fra 2 may be able to assist cluster transfer of Grx4 to Php4 in a similar fashion, however, adding Fra2 from *S. cerevisiae* did not cause this conversion to occur. In order to test whether an additional protein was required to assist in this transfer, an extract from *S. pombe* was added. Again, no transfer occurred, although it could be due to a low concentration of the required protein. Previous work found that the holo Grx4-Php4 heterodimer was thermodynamically favored over Grx4 homodimer since Grx4-Php4 was added to excess Grx4 the resultant UV-visible and CD spectra did not resemble those of Grx4 homodimers found in other species. Also, Grx4 and Php4 constitutively interact regardless of iron binding. It is thought that an additional iron delivery protein is used to bring an [2Fe-2S] cluster to the apo Php4-Grx4 complex (Vachon et al, 2012). The protein involved as well as the mechanism of transfer of the cluster are still unknown. (Dlouhy, 2015). My work sought to purify *S. pombe* Fra2 to use as a cofactor to transfer cluster from Grx4 homodimer to the Php4-Grx4 complex, but Fra2 was often insoluble and unstable. Coexpressing Fra2 with Pphp4 or Grx4 did not improve the stability. A urea extraction of Fra2 expressed independently improved solubility but Fra2 was still unstable. Fra2 coexpressed with the Takara chaperones did not improve the solubility.

Materials and Methods

Strains and Plasmids. For all plasmid preps, plasmids were grown in DH5α *E. coli* strains and for expression all plasmids were grown in BL21(DE3) *E. coli* strains. The pJK210-fra2 ORF plasmids were generously provided by Dr. Simon Labbé and cloned into pET21a vector. A truncated version of the plasmid with amino acids 1-76 was used for the listed experiments. Coexpression of Fra2 was done with pRSFDuet-1 + Php4, pRSFDuet-1 + Grx4 and pRSFDuet-1 + Php4/Grx4 plasmids. The Takara chaperone plasmids were provided by Makris lab and transformed into pET21a + pJK210-fra2.

Purification methods of Fra2 Plasmids were grown in BL21(DE3) *E. coli* cells and induced with isopropyl β-D-1-thiogalactopyranosid (IPTG) and grown at 37 °C. Cells were lysed through 5 freeze/thaw cycles, and/or sonication then purified on a HiPrep 16/10 DEAE FF ion exchange column with 50 mM Tris pH 8.0 and a 100 mL 1 M NaCl gradient, followed by a GE HiPrep Phenyl FF hydrophobic interaction column using 50 mM Tris pH 8.0, and separated on a GE HiLoad Superdex 75 size exclusion column in 50 mM Tris pH 8.0 + 150 mM NaCl. (Dlouhy, 2015).

Urea Extraction of Fra2 pET21a + pJK210-fra2 was induced with 0.5 mM IPTG at 30 °C then cells were resuspended in 50 mM Tris pH 7.5 and put through 5 cycles of freezing and thawing. Protease inhibitors were added and cells were sonicated. The resultant pellet was resuspended in Tris buffer + 8 M Urea + 20 mM DTT and stirred at room temperature for 1 hour. The sample was centrifuged at 16,000 rpm for 20 min and the supernatant was put in snakeskin for dialysis placed in 1 L of Tris buffer + 0.5 M Urea + 2 mM DTT and stirred uncovered a 4 °C for 2 hours. The dialysis solution was moved to 2 L of Tris buffer + 2 mM DTT and stirred covered at 4 °C overnight. The product of

the dialysis was purified on a DEAE ion exchange column using 50 mM Tris pH 7.5 and fractions were concentrated using a 3K concentrator. The protein was loaded on the Superdex 75 size exclusion column but degraded during loading.

Results and Discussion

A truncated version of the Fra2 protein was provided by the Labbé lab and transformed into competent *E. coli* cells. pRSFDuet-1+Php4+, pRSFDuet-1+Grx4+Fra2, and pRSFDuet-1+Php4/Grx4+Fra2. were transformed into competent BL21(DE3) cells. Some combinations of transformations were unsuccessful, but strains were finally transformed successfully when using competent BL21(DE3) cells containing a pRSFDuet-1+Php4+, pRSFDuet-1+Grx4+Fra2, and pRSFDuet-1+Php4/Grx4+Fra2 were transformed in via electroporation. Two colonies of each transformation type were screened to optimize induction at 0.6 OD with 0.5 mM IPTG and grown overnight at 30 °C (Figure 3.1). The results of the pRSFDuet-1+Php4 + Fra2 colonies showed Php4 was very soluble and Fra2 was somewhat soluble. From these results, it is likely there is no interaction between Php4 and Fra2. This strain was able to be grown at a larger scale using the pre-mentioned induction parameters. The both Grx4 and Fra2 were slightly soluble in pRSFDuet-1+Grx4 + Fra2. The induction parameters were further optimized using 0.5 mM IPTG or 20µM IPTG and grown overnight at either 16 °C or 25 °C (Figure 3.2). The results of 20 µM IPTG and 25 °C had the best expression. The pRSFDuet-1+Grx4/Php4 + Fra2 strain had very soluble Php4 but less soluble Grx4 and Fra2. This suggests that the Grx4-Fra2 complex is most likely preferred over the Php4-Fra2 complex. Php4 has previously had reduced solubility when expressed with Grx4, it can be assumed no interaction occurs

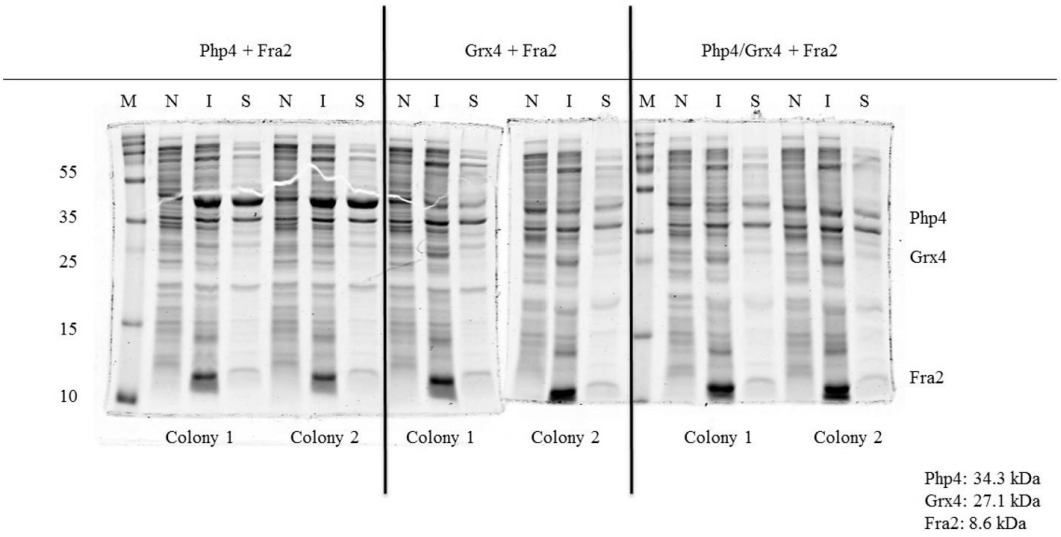

Figure 3.1 Induction parameters test on co-expression colonies. Small scale inductions tests completed by adding 0.5 mM IPTG at OD=0.6 and grown overnight at 30 °C. M indicates a protein plus marker, N, non-induced cells, I, induced cells, and S, the soluble fractions treated with B-PER.

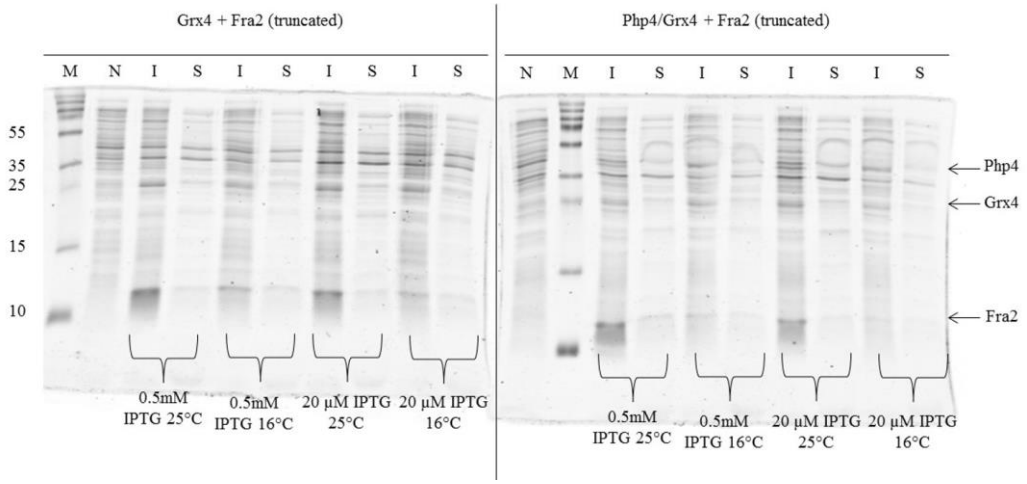

Figure 3.2 Additional induction tests. Induction parameters were optimized by testing expression under listed conditions. M indicates a protein plus marker, N, non-induced cells, I, induced cells, and S, the soluble fractions treated with B-PER.

between Php4 and Grx4 or Php4 and Fra2 when all three proteins are coexpressed. To increase solubility of Fra2, the induction parameters were tested as previously mentioned, and 20 µM IPTG and 25 °C provided the best expression.

pRSFDuet-1+Php4 + Fra2 was purified in 1 L culture induced at 0.6 OD with 0.5 mM IPTG and grown overnight at 30 °C and sonicated aerobically. Then purified by ion exchange chromatography (Figure 3.3) followed by size exclusion chromatography. No Fra2 was present due to loss or degradation. In pRSFDuet-1+Grx4 + Fra2, Fra2 was found to be insoluble (Figure 3.4). In the pRSFDuet-1+Php4/Grx4 + Fra2, Fra2 was present after ion exchange chromatography, but was degraded when purified on a hydrophobic interaction column (Figure 3.5 and 3.6).

pET21a + pJK210-fra2 was induced with 0.5 mM IPTG at 30 °C then sonicated and separated by ion exclusion followed by hydrophobic interaction chromatography. Fra2 was lost (Figure 3.7) during this procedure. Insoluble Fra2 was found in the initial pellet after lysis, so a urea extraction was done on the insoluble portion, but the protein was unstable and degraded.

pET21a + pJK210-fra2 was transformed using the Takara chaperone proteins that were graciously donated to us from Dr. Tom Makris. Each chaperone plasmid was transformed with pET21a + pJK210-fra2 (Figure 3.8) and induced with 0.5 mM IPTG and according to the Takara protocol. Induction was optimized, however, the increase of Fra2 solubility was minimal. Stocks of the Takara plasmids with Fra2 plasmid were stored in Kirsten's box at -70 °C.

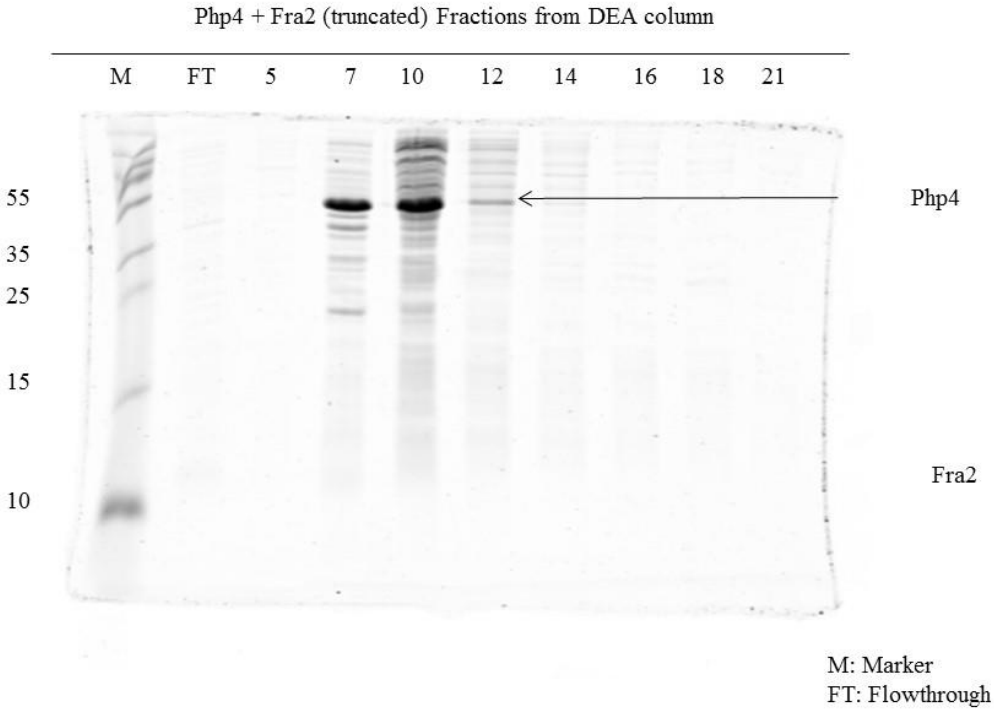

Figure 3.3 Php4 + Fra2 DEAE fractions. Php4 was present in fractions 7 through 12 but Fra2 was either insoluble or degraded.

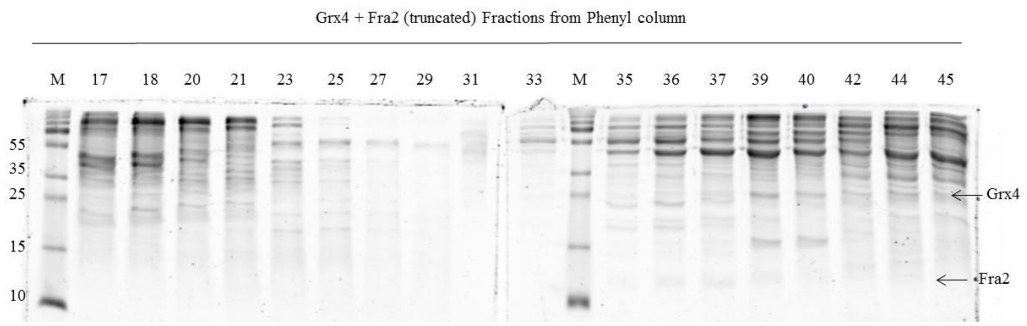

Figure 3.4 Grx4 + Fra2 fractions from phenyl column. Grx4 has low solubility but Fra2 is either insoluble or degraded.

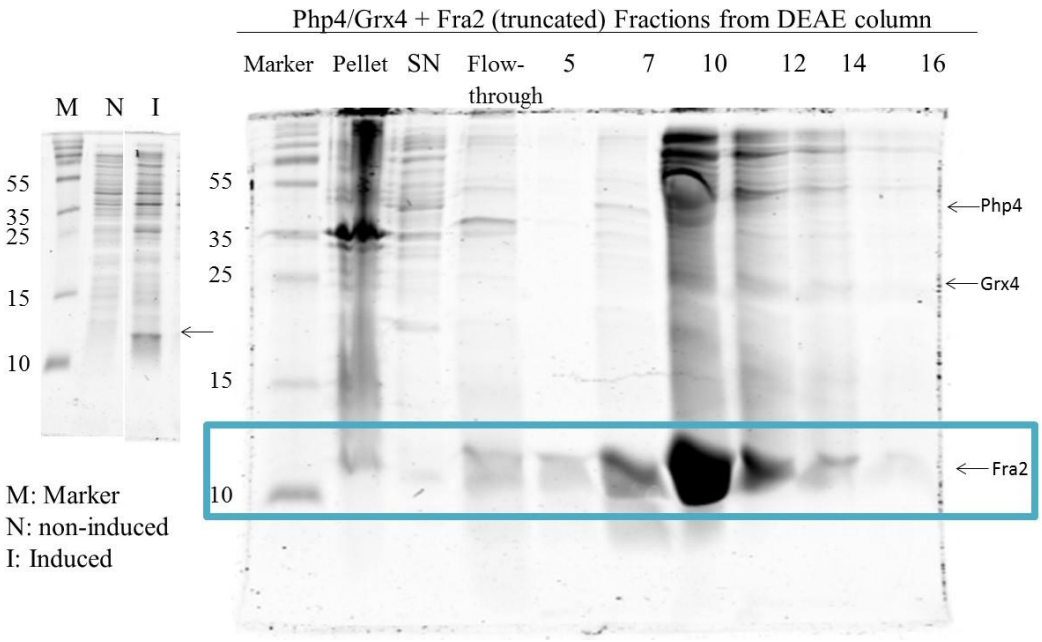

Figure 3.5 Php4/Grx4 + Fra2 DEAE fractions. All three proteins are soluble and Fra2 has high expression and solubility. Fractions 5-12 were concentrated.

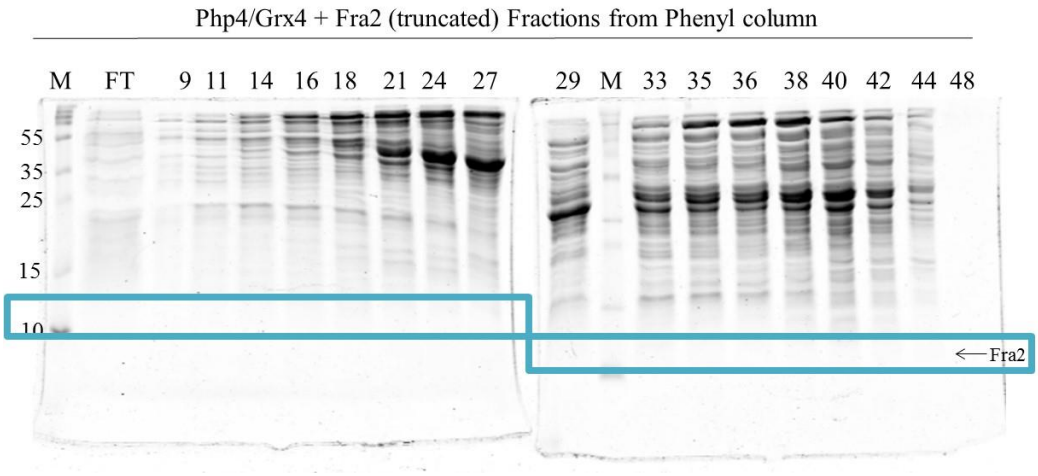

Figure 3.6 Php4/Grx4 + Fra2 phenyl fractions. Fra2 was degraded or lost.

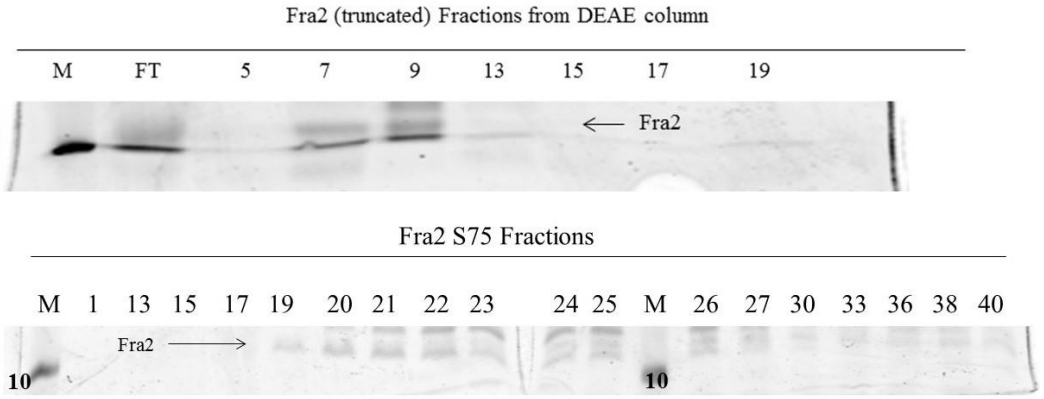

Figure 3.7 Fra2 DEAE and phenyl fractions. Fra2 was not very soluble and was unstable following the phenyl column purification.

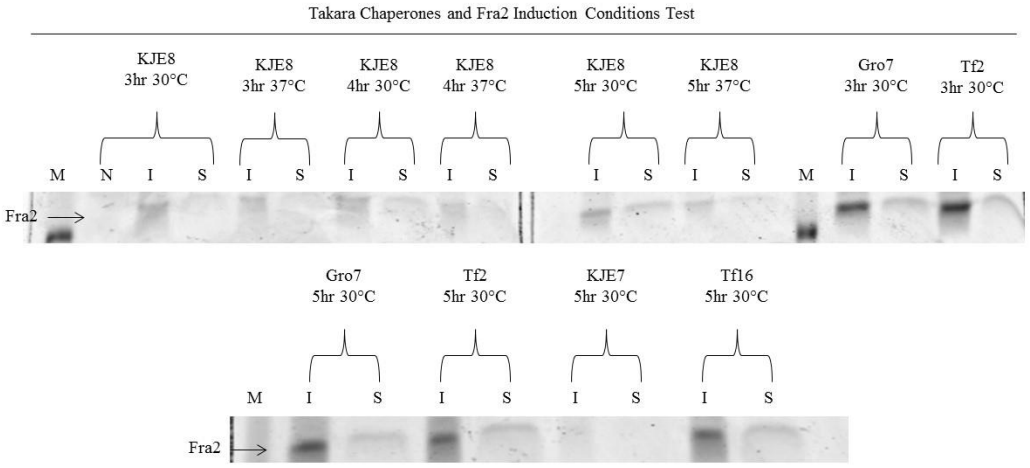

Figure 3.8 Takara chaperones induction parameters. Each chaperone protein was transformed and co-expressed with Fra2 under the indicated conditions.

The purification of Fra2 when coexpressed with Php4 as well as when coexpressed with Php4 and Grx4 was able to successfully purify Php4, but Fra2 was not found in the final fractions due to loss or lack of stability. Purification of Fra2 in the pRSFDuet-1+Grx4+Fra2 strain found that the Fra2 protein was not soluble and was found only in the pellet formed after lysing. Purification of pET21a + pJK210-fra2 found Fra2 to be unstable leading to the degradation of Fra2 during purification procedures. Future experiments should include more stabilization of Fra2 in order to purify the protein. Purified protein can be used as a cofactor to test the transfer of a cluster from Grx4 to Php4.

Chapter 4

Measuring the impact of glutathione overaccumulation on subcellular redox balance

Abstract

Glutathione is essential in reducing reactive oxygen species (ROS) and maintaining redox balance within the cell. A rxYFP sensor was targeted to the mitochondrial intermembrane space (IMS) in order to measure the redox states of this subcellular compartment when the cell was exposed to oxidative stress. Previous experiments found that the redox sensor was about 70% oxidized when the glutathione importer, Hgt1, was overexpressed and GSH was added to the media. In an effort to replicate this experiment, I was met with unexpected results and much troubleshooting that is still in the process of being resolved. I am hoping to perfect this experiment in order to answer questions about the redox states and mechanisms controlling redox homeostasis on the subcellular level.

Introduction

Normal functions within eukaryotic cells leads to the formation of reactive oxygen species (ROS). Glutathione (GSH) helps to regulate thiol-disulfide balance by converting between its reversible reduced (GSH) and oxidized (GSSG) forms. Glutathione is also

essential for protection against oxidative stress that can occur due to the exposure of carcinogens, xenobiotics or radiation. (Grant CM 1996). Endogenous GSH is synthesized in two steps, by GSH1 (gamma-glutamycysteine synthase) and GSH2 (glutathione synthetase). In addition to being synthesized in the cell, GSH may be imported from extracellular environment by Hgt1p, a high affinity glutathione transporter. (Bourbouloux et al. 2000). Cellular redox changes can affect many processes within the cell such as enzymatic function or protein interactions. Therefore, it is important that redox homeostasis is maintained within the cells. One way to monitor redox changes in vivo is with redox sensors. Two that are relevant to the work in this lab are roGFP2 and rxYFP. These sensors were created so they are able to form a reversible disulfide bond on the surface of the sensor (Figure 4.1) (Sugiura et al 2015). The genetically-encoded sensors can be targeted to different subcellular compartments using organelle-specific targeting sequences (Figure 4.2). Our lab is able to monitor this sensor in its reduced and oxidized forms through a non-reducing SDS-PAGE gel due to different electrophoretic mobilities between the two forms.

In our lab it has been shown previously that mitochondrial and cytosolic rxYFP sensors selectively register redox variations within subcellular compartments. The model system, *S. cerevisiae*, was subjected to severe stress by overexpressing glutathione transporter, Hgt1 which has been shown to result in higher levels of GSH and GSSG upon addition of glutathione to the media (Kumar, et al., 2011). The IMS was found to have a separate glutathione pool that maintains redox homeostasis under severe stress (Darch, 2015).

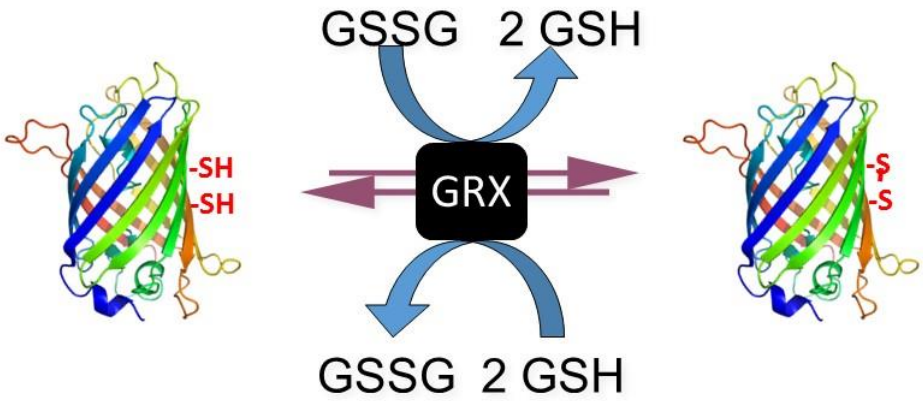

Figure 4.1 rxYFP sensor. Sensor is able to form reversible disulfide bond which equilibrates to the local GSH:GSSG redox environment. A glutaredoxins allows this equilibration to occur more quickly but may influence the redox environment. Figure from C. Outten.

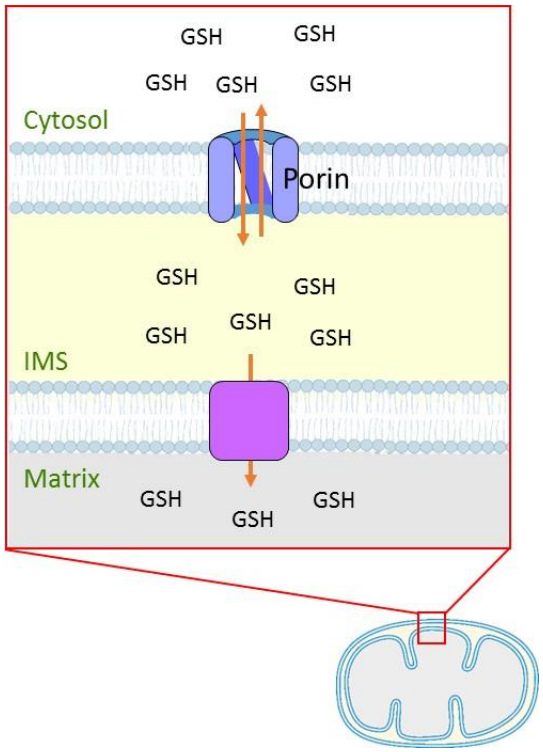

Figure 4.2 Mitochondrial intermembrane space. Glutathione is transported from the cytosol into the intermembrane space (IMS) and mitochondrial matrix by transport proteins. The redox sensor has a targeting sequence which localizes the sensor in the IMS. Figure from C. Outten.

Materials and Methods

Plasmids and Strains Strains were maintained at 30 °C on synthetic complete medium (SC) supplemented with 2% glucose and the necessary amino acids. The cytosol- (pHOJ150) and IMS-rxYFP (pJH200) expression plasmids and IMS-Glr1 plasmid, pJH313, was constructed by Jingjing Hu (Hu, 2010). The plasmid pTEF416-HGT1 having constitutive expression of HGT1 was constructed by Maxwell Darch (Darch, 2015).

TCA precipitation Cells were grown on SC selection -Ura, -Leu plates for 1 day from a -70 °C freezer stock. Overnight cultures from the plate were started in 20 mL selection media at 30 °C shaking so the OD600 is below1 the following morning then fresh cultures were started from overnight cultures and grown about 3 hours to an OD600 of 0.2. Transfer 5 OD600 into a 50 mL conical tube and add 100% ice-cold TCA to the cells to make the final concentration 15%. Incubate on ice for 10 minutes. Time 0 aliquot was removed before adding GSH (100 µM) or GSSG (50 µM). Cells were harvested by centrifugation at 3k rpm for 5 minutes. SN poured off and pellet resuspended in 1 mL ice-cold 10% TCA. Samples transferred to a microcentrifuge tube and kept on ice. 1 mL glass beads added and cells lysed in Mini bead beater 16 (Biospec). using 2 2-minute pulses in the cold room. SN transferred to a new microcentrifuge tube and spun at 13 k rpm 5 min (4°C), and SN aspirated. Samples were stored at -70 °C up to 5 days. 250 µL 1X SDS loading buffer (no DTT) + 40 mM NEM was added and cells incubated at RT for 10 minutes. 30 µL of samples were loaded on a 16% Tris-glycine gel (Invitrogen) and run at 145 V for 3 hours and 45 minutes (Newer gels only need to run about 2 hours and 30 minutes). Gel was transferred to a nitrocellulose membrane at 25V for 1.5 hours.

Immunoblotting Techniques Whole cell yeast extracts were analyzed by Western blotting using an anti-GFP (Invitrogen) antibody and a secondary anti-rabbit IgG (IRDye, LI-COR Lincoln, NE). Western blots were analyzed using an Odyssey Infrared Imaging System (LI-COR).

Results and Discussion

The plasmid used contains a mitochondrial intermembrane space (IMS) targeted rxYFP sensor to measure the GSH:GSSG ratio over time in a strain which overexpresses Hgt1 importer. The IMS-rxYFP sensor on the pJH200 plasmid (Hu, 2010) was transformed into pTEF416 HGT1 overexpression strain and an empty vector control. Previous experiments in our lab, (Darch, 2015) which found that the redox sensor was about 70% oxidized after GSH was added to the HGT1 overexpression strain, were repeated with additional time points: 0, 1, 5, 15, 30, 60, 120, and 240 minutes after GSH or GSSG addition (Figure 4.3). Using stocks of previously made strains, the sensor was less than 30% oxidized (Vector) or between 20 and 15% oxidized (HGT1) across all time points. The experiment was repeated keeping all ODs under 1 at all times. This had no effect, the strains were still reduced. Multiple freezer stocks made previously by Max or Jingjing were tested at the zero time point only (Figure 4.4) but no change in oxidation was observed. The pJH200 plasmids were retransformed into pTEF416 strains. The resultant colonies were tested at the zero-time point (Figure 4.5). The H1 colony and the V1 colony were both around 50% oxidized while all other strains were less oxidized. These two strains were used in all additional experiments. The effectiveness of the rxYFP sensor was compared to the IMS-rxYFP sensor and a cytosolic rxYFP sensor in a *glr1*Δ strain with the

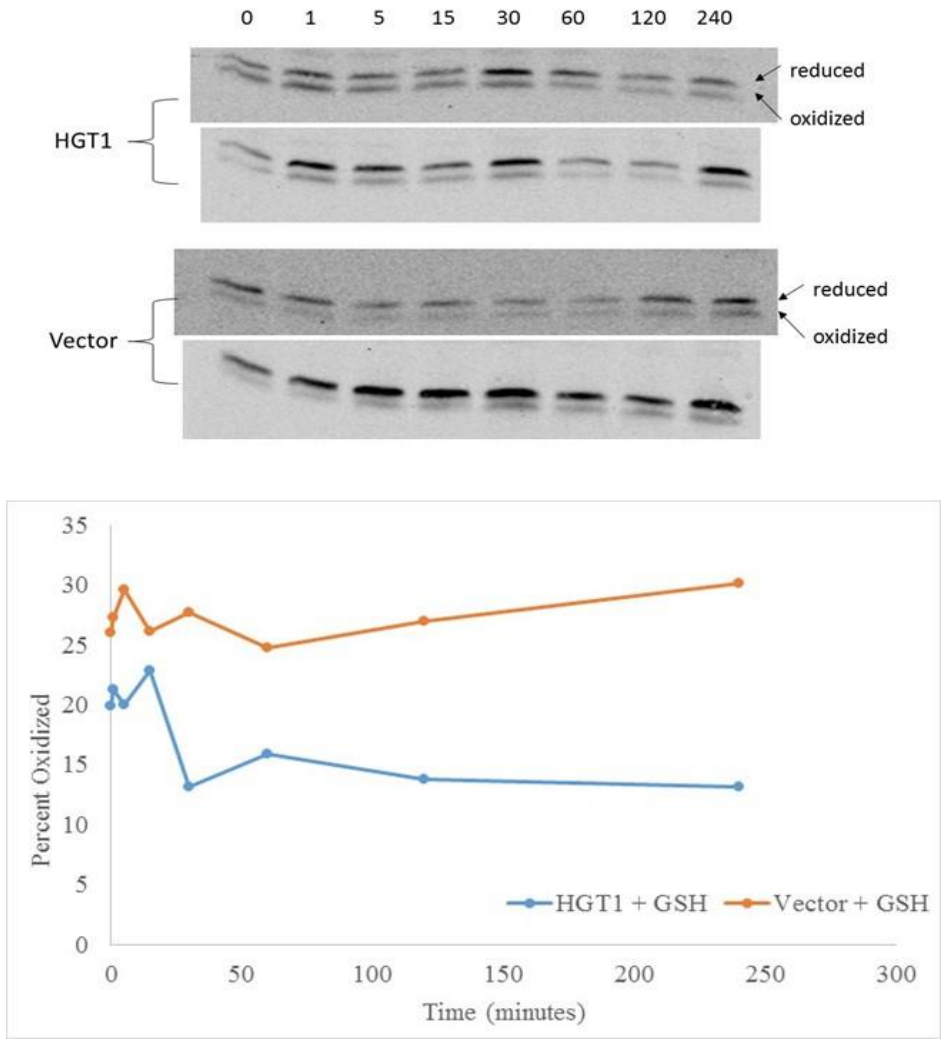

Figure 4.3 IMS-rxYFP sensor in HGT1 overexpression strain. The IMS-rxYFP sensor on the pJH200 plasmid in the pTEF416 HGT1 overexpression strain and the empty vector control measured over time after the addition of 100mM GSH.

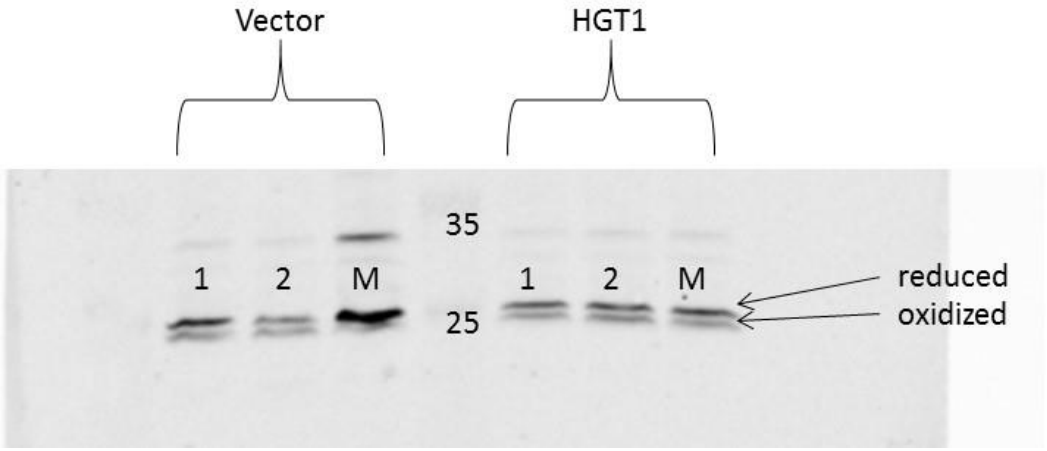

Figure 4.4 IMS-rxYFP sensor in multiple strains. The IMS-rxYFP sensor on the pJH200 plasmid in the pTEF416 HGT1 overexpression strain and the empty vector control measured without glutathione. 1 and 2 represent colonies of strains created by Dr. Jingjing Hu, M represents new transformants of the same strains created by Dr. Maxwell Darch.

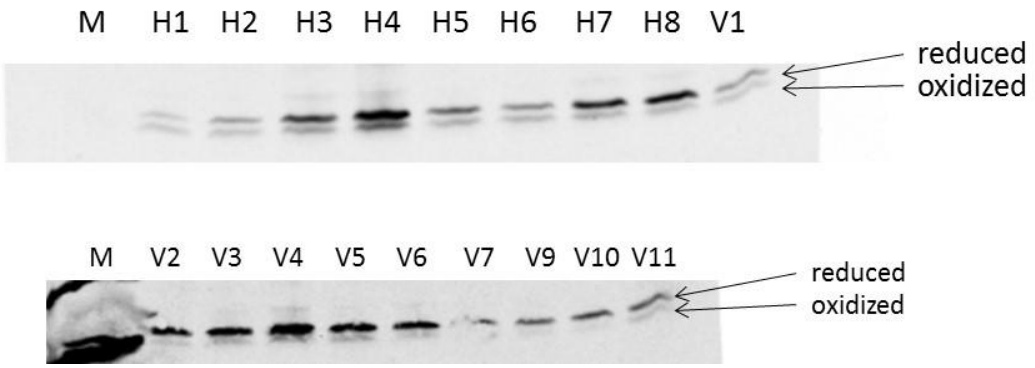

Figure 4.5 IMS-rxYFP sensor in newly transformed strains. The IMS-rxYFP sensor on the pJH200 plasmid in the pTEF416 HGT1 overexpression strain and the empty vector control measured without glutathione. H1 and V1 are the most oxidized at about 50%.

corresponding wild type controls (Figure 4.6). IMS-rxYFP was 44% oxidized in the WT strain and 53% oxidized in *glr1*Δ and Cytosol-rxYFP is 20% oxidized in WT and 87% oxidized in *glr1*Δ, which corresponds to previous data (Hu, 2010) (Figure 4.7). The most interesting observation was that the HGT1 strain was now mostly oxidized for an unknown reason.

The reason for the change in HGT1 was hypothesized to be due to a slightly different OD when samples were extracted. A test of multiple ODs was completed and all samples were mostly oxidized and no conclusion could be made (Figure 4.7). The experiment at all the time points was repeated using an OD of 0.2-0.3. The sensor was more than 70% oxidized at all ODs. Another troubleshooting experiment tested sample preparation parameters (Figure 4.8). It compared normal treatment to the following changes: An additional vortex step added after TCA addition to ensure all thiols were trapped, freezing of the pellet was eliminated, time on ice after TCA addition was doubled to 20 minutes, 1M Trizma was doubled to 20µL, SDS buffer was reduced to concentrate samples, and the pellet was vortexed after Trizma addition. In addition, a separate iodoacetamide (IAM) trapping approach (Bouldin, 2010) was compared to the normal TCA precipitation with NEM modification (Figure 4.9). None of the changes had significant effects. The assay was completed twice and the quantifications were averaged (Figure 4.10). The HGT1 strain is 55% oxidized and drops to 30% oxidized compared to previous experiments (Darch, 2015) showing a 70% oxidation dropping rapidly to about 40% oxidized before recovering slightly over time. The vector strain was 40% oxidized increasing to 65% oxidized compared to 70% oxidized in previous experiments.

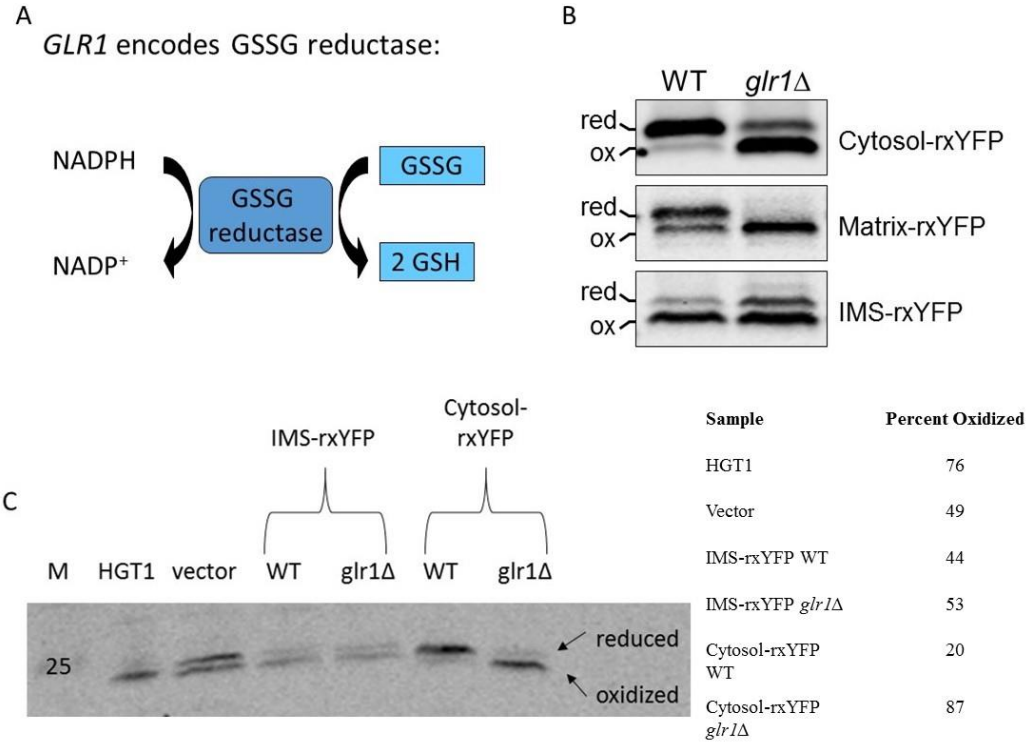

Sample	Percent Oxidized
HGT1	76
Vector	49
IMS-rxYFP WT	44
IMS-rxYFP *glr1*Δ	53
Cytosol-rxYFP WT	20
Cytosol-rxYFP *glr1*Δ	87

Figure 4.6 Test of rxYFP sensor in HGT1 and *glr1*Δ. Glr1 is glutathione reductase which uses NADPH as a cofactor to reduce GSSG to GSH (A). Previous studies (Hu, 2010) have shown that the cytosolic and IMS sensors in *glr1*Δ are mostly oxidized but the cytosolic sensor in the wild type strain is mostly reduced (Figure from Hu, 2010) (B). The IMS-rxY1FP sensor on the pJH200 plasmid in the pTEF416 HGT1 overexpression strain was compared to the IMS-rxYFP sensor and the cytosol-rxYFP sensor in the *glr1*Δ strain(C).

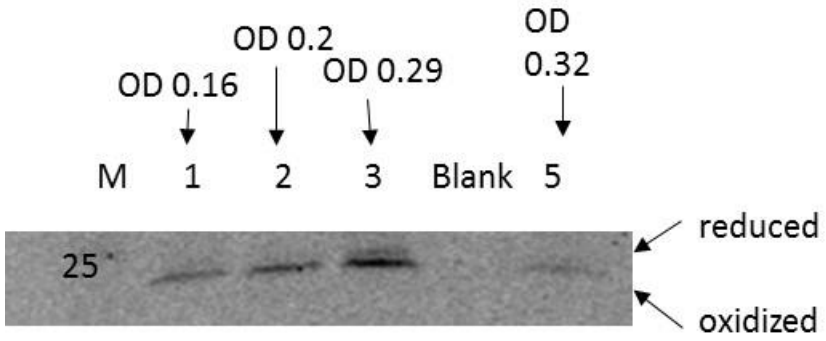

Figure 4.7 OD optimization of rxYFP sensor in HGT1. The IMS-rxYFP sensor in the HGT1 overexpression strain grown to different optical densities. Measurements at all ODs were greater than 70% oxidized.

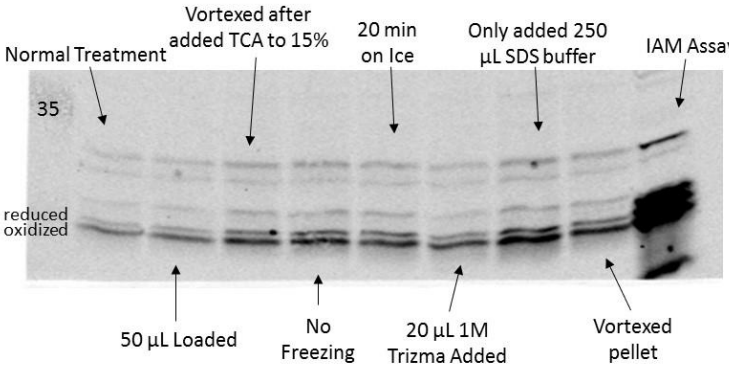

Change	Percent Oxidized
Normal	71.2
50 µL Loaded	66.1
Vortexed TCA	57.6
No Freezing	61.3
20 min ice	68.3
Trizma	68.3
250 µL Buffer	65.6
Vortexed Pellet	(right band was too dark)
IAM Assay	(bands too close)

Figure 4.8 Troubleshooting of rxYFP sensor in HGT1. The IMS-rxYFP sensor in the HGT1 overexpression strain prepared as indicated. Quantification done on the Li-Cor Odyssey.

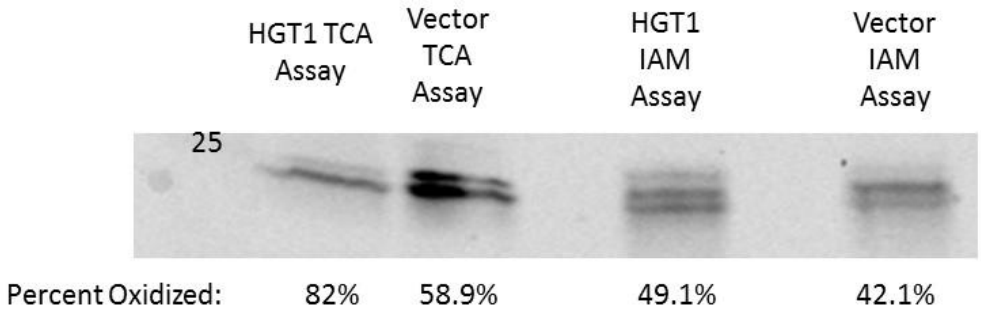

Figure 4.9 Iodoacetamide assay of rxYFP sensor in HGT1. Iodoacetamide (IAM) assay completed following protocol (Bouldin, 2010). Compared to TCA precipitation. Quantification done on the Li-Cor Odyssey.

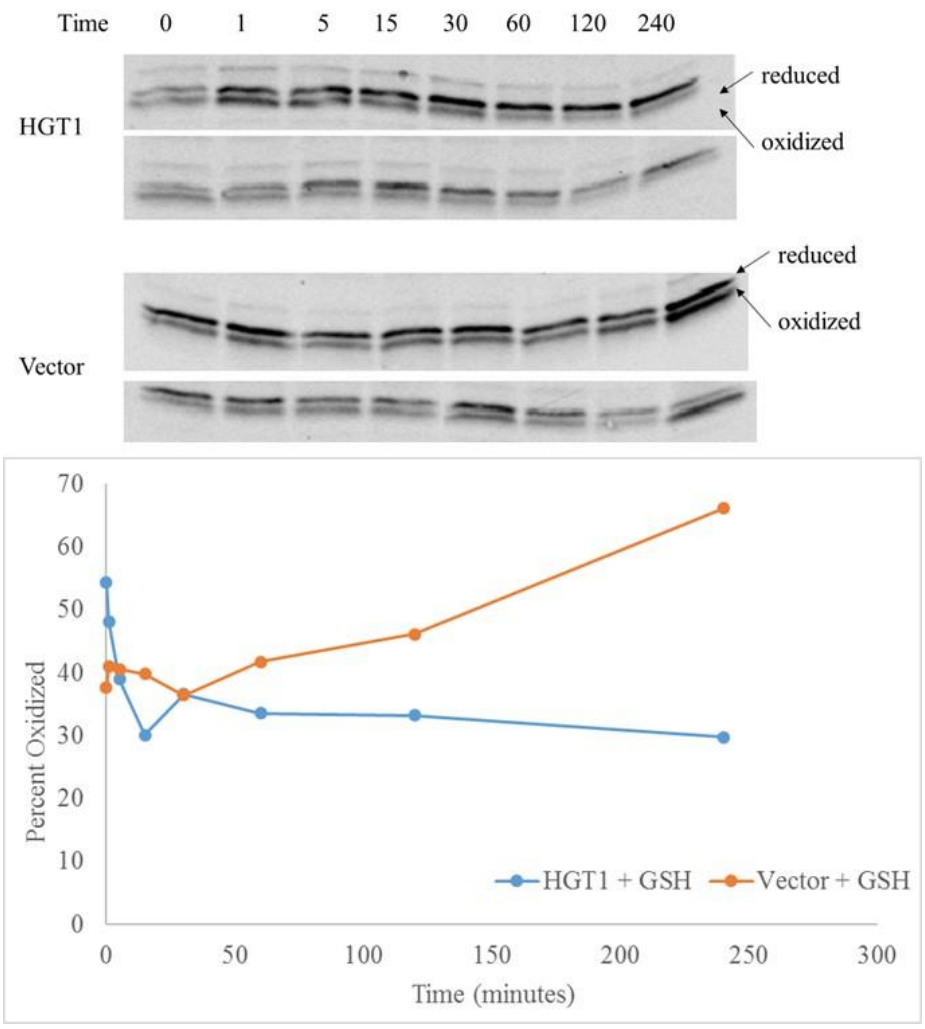

Figure 4.10 IMS-rxYFP sensor in HGT1 with added Glutathione. 50mM GSH added. Average of two assays each strain. Quantification done on the Li-Cor Odyssey.

It was seen multiple times that the sensor was very reduced after the addition of either reduced or oxidized glutathione. This could be due to reduced visibility due to low concentrations in the westerns. More troubleshooting and additional experiments need to take place in order to confidently report the oxidation of the redox sensor when exposed to glutathione.

Chapter 5

Supplementary Methods

Introduction

This chapter provides details of materials and new methods created or altered to achieve the results presented in this thesis. This includes growth of galactose-regulated strains, TCA precipitation for redox western updates, and a table of all strains used.

Growth of galactose-regulated strains

All growth was started on synthetically defined (SD) media with all amino acids, 50µM $FeCl_3$ and 2% galactose. Strains were grown 2 to 3 days on plates from freezer stocks (Kirsten's box) at 30°C. Cells were then moved to liquid SD media with 2% galactose and grown overnight. ODs were kept between 1-2. Cultures were grown at 30°C in shaking incubator. After 24 hours, cells were collected, washed twice with 1 mL sterile water and resuspended in media containing 2% glucose. The following changes were made over the course of this project:

1. Culture ODs kept below 1 OD

a. Strains were started at very low ODs (around 0.001) and allowed to grow to around 0.2-0.6 OD. Cultures were systematically diluted to keep ODs under 1. Samples were taken when OD=0.2.

2. Cells grown with and without $FeCl_3$ (50µM).
3. Cells were grown in a non-shaking incubator at 30°C to reduce oxidative stress
    a. Grown in 50 mL cultures in the incubator in GSRC 306. Cells grew much slower.
4. 2% raffinose was substituted for glucose
    a. Some experiments grew in 2% Galactose to 2% Raffinose, but others used 0.5% Galactose plus 2% Raffinose to only Raffinose or only Glucose.
5. The wash step was removed so that the galactose was removed over time
    a. Cultures were diluted into the new media at a calculated OD. This only caused the suppressor mutation to develop later.

TCA precipitation for redox western

Original procedure located on page 132 Darch, 2015. The following changes were made:

1. Cells were grown on a plate overnight before starting liquid cultures. (Always take cells from freezer stocks)
2. The empty vector grows much faster than the HGT1 strain, so I typically grow 2 mL of vector and 100 mL of HGT1 overnight to an OD of 0.6-1. (No higher

than 1). Then I dilute in the morning to 0.1 (HGT1) and 0.05 (vector) and grow about 3 hours to an OD of 0.2.

3. Only the 250 µL SDS with 40 mM NEM was added to the samples. The additional 250 µL of buffer was omitted.
4. For the newer 16% gels only run about 2.5 hours or until the green band runs off the gel.

Table 5.1 Strains and plasmids used.

Strain/Plasmid	Genotype	Reference
BY4742	*MATα his3Δ1 leu2Δ0 lys2Δ0 ura3Δ0*	Mulenhoff et. al., 2010
W303-1A	*MATa ura3-1 ade2-1 trp1-1 his3-11,15 leu2-3,112*	Mulenhoff et. al., 2010
grx3Δgrx4Δ	BY4742 *grx3::LEU2; grx4::KanMX4*	Mulenhoff et. al., 2010
grx3Δ Gal-*GRX4*	W303-1A *pGRX4::GAL-L-natNT; grx3::LEU2*	Mulenhoff et. al., 2010
BY4742	*MATα his3Δ1 leu2Δ0 ura3Δ0*	Dancis, unpublished
grx4Δ Gal-*GRX3*	BY4742 *Δgrx4::KanMX His3MX6-pGAL1-3HA-GRX3*	Dancis, unpublished
pJK210-fra2 + without stop codon		Labbé, unpublished
BY4741 WT + pTEF416 HGT1 + pJH200	(BY4741); pTEF416 HGT1; pJH200	Darch, 2015; Hu, 2010
BY4741 glr1Δ + pTEF416 Vector + rxYFP-IMS	(BY4741); pTEF416 Vector; pJH200	Darch, 2015; Hu, 2010
pJH200+pTEF416 (BY4741)	MATa his3Δ1 leu2Δ0 met15Δ0 ura3Δ0; pHOJ150 cyb2-rxYFP; pTEF416	Hu, 2010
pJH200+pTEF416-HGT1 (BY4741)	MATa his3Δ1 leu2Δ0 met15Δ0 ura3Δ0; pHOJ150 cyb2-rxYFP; pTEF416 HGT1	Hu, 2010
BY4741 glr1Δ + pTEF416 HGT1 + rxYFP-Cytosol	(BY4741) pTEF416 HGT1; pHOJ150 (rxYFP-Cytosol)	Hu, 2010

References

Askwith, C., & Kaplan, J. (1998). Iron and copper transport in yeast and its relevance to human disease. *Trends in biochemical sciences, 23*(4), 135-8.

Bandyopadhyay, S., Chandramouli, K., & Johnson, M. K. (2008). Iron-sulfur cluster biosynthesis. *Biochemical Society transactions, 36*(Pt 6), 1112-9.

Bandyopadhyay, S., Gama, F., Molina-Navarro, M., Gualberto, J., Claxon, R., Naik, S., . . . Rouhier, N. (2008). Chloroplast monothiol glutaredoxins as scaffold proteins for the assembly and delivery of [2Fe-2S] clusters. *EMBO J, 27*, 1122-1133.

Baudouin-Cornu, P., Lagniel, G., Kumar, C., Huang, M. E., & Labarre, J. (2012). Glutathione degradation is a key determinant of glutathione homeostasis. *The Journal of biological chemistry, 287*(7), 4552-61.

Bouldin, S. (2010) Characterizing Factors that Influence Intracellular Thiol-disulfide Equilibrium, In Chemistry and Biochemistry, p 97, University of South Carolina, UMI Dissertation Publishing.

Darch, M. (2015) Subcellular Glutathione Distribution During Severe Redox Stress and Characterizing Thiol Redox Control of Human Cu, Zn Superoxide Dismutase, In Chemistry and Biochemistry, p73, University of South Carolina, UMI Dissertation Publishing.

Dlouhy, A. (2015) Illuminating the Interactions and Functions of Glutaredoxins, BolA Proteins, and Erv1 in Iron Homeostasis, In Chemistry and Biochemistry, p 113-146, University of South Carolina, UMI Dissertation Publishing.

Hu, J. (2010) Investigating Subcellular Thiol Redox Chemistry with GFP-based Redox Sensors, In Chemistry and Biochemistry, p 175, University of South Carolina, UMI Dissertation Publishing.

Hu, J., Dong, L., and Outten, C. E. (2008) The redox environment in the mitochondrial intermembrane space is maintained separately from the cytosol and matrix, The Journal of biological chemistry 283, 29126-29134.

Iwema, T., Picciocchi, A., Traore, D. A., Ferrer, J. L., Chauvat, F., & Jacquamet, L. (2009). Structural basis for delivery of the intact [Fe2S2] cluster by monothiol glutaredoxin. *Biochemistry, 48*(26), 6041-3.

Jacques, J.-F., Mercier, A., Brault, A., Mourer, T., & Labbe, S. (2014). Fra2 is a co-regulator of Fep1 inhibition in response to iron starvation. *PLoS One, 9*(6), e98959.

Kolossov, V. L., Hanafin, W. P., Beaudoin, J. N., Bica, D. E., DiLiberto, S. J., Kenis, P. J., & Gaskins, H. R. (2014). Inhibition of glutathione synthesis distinctly alters mitochondrial and cytosolic redox poise. *Experimental Biology and Medicine, 239*, 394-403.

Kumar, C., Igbaria, A., D'Autreaux, B., Planson, A. G., Junot, C., Godat, E., Toledano, M. B. (2011). Glutathione revisited: a vital function in iron metabolism and ancillary role in thiol-redox control. *The EMBO journal, 30*(10), 2044-56.

Labbé, S. K. (2013). Iron uptake and regulation in Schizosaccharomyces pombe. *Curr. Opin. Microbiol, 16*, 669-676.

Li, H., & Outten, C. (2012). Monothiol CGFS Glutaredoxins and BolA-like Proteins: [2Fe-2S] Binding Partners in Iron Homeostasis. *Biochemistry, 51*(22), 4377-4389.

Li, L., Bogley, D., Ward, D.M., & Kaplan, J. (2008). Yap5 is an iron-responsive transcriptional activator that regulates vacuolar iron storage in yeast. *Mol Cell Biol, 28*, 1326-1337.

Li, L., Jia, X., Ward, D. M., & Kaplan, J. (2011). Yap5 protein-regulated transcription of the TYW1 gene protects yeast from high iron toxicity. *J Biol Chem, 286*, 38488-38497.

Mercier, A., Pelletier, B., & Labbé, S. (2006). A transcription factor cascade involving Fep1 and the CCAAT-binding factor Php4 regulates gene expression in response to iron deficiency in the fission yeast *Schizosaccharomyces pombe*. *Eukaryot Cell, 5*, 1866-1881.

Mercier, A., Watt, S., Bähler, J., & Labbé, S. (2008). Key function for CCAAT-binding factor Php4 to regulate gene expression in response to iron deficiency in fission yeast. *Eukaryot Cell, 7*, 493-508.

Muhlenhoff, U., Molik, S., Godoy, J. R., Uzarska, M. A., Richter, N., Seubert, A., . . . Lill, R. (2010). Cytosolic monothiol glutaredoxins function in intracellular iron sensing and trafficking via their bound iron-sulfur cluster. *Cell metabolism, 12*(4), 373-85.

Ojeda, L., Keller, G., Muhlenhoff, U., Rutherford, J. C., Lill, R., & Winge, D. R. (2006). Role of glutaredoxin-3 and glutaredoxin-4 in the iron regulation of the Aft1 transcriptional activator in Saccharomyces cerevisiae. *The Journal of biological chemistry, 281*(26), 17661-9.

Outten, C. E., & Albetel, A. N. (2013). Iron sensing and regulation in Saccharomyces cerevisiae: Ironing out the mechanistic details. *Current opinion in microbiology, 16*(6), 662-8.

Pelletier B, B. J. (2002). Fep1, an iron sensor regulating iron transporter gene expression in Schizosaccharomyces pombe. *J Biol Chem, 277*(25), 22950-8.

Poor, C. B., Wegner, S. V., Li, H., Dlouhy, A. C., Schuermann, J. P., Sanishvili, R., . . . He, C. (2014). Molecular mechanism and structure of the Saccharomyces cerevisiae iron regulator Aft2. *Proceedings of the National Academy of Sciences of the United States of America, 111*(11), 4043-8.

Pujol-Carrion, N., & de la Torre-Ruiz, M. A. (2010). Glutaredoxins Grx4 and Grx3 of Saccharomyces cerevisiae play a role in actin dynamics through their Trx domains, which contributes to oxidative stress resistance. *Applied and environmental microbiology, 76*(23), 7826-35.

Toledano, M. B., Delaunay-Moisan, A., Outten, C. E., & Igbaria, A. (2013). Functions and cellular compartmentation of the thioredoxin and glutathione pathways in yeast. *Antioxidants & redox signaling, 18*(13), 1699-711.

Zimmermann, M. B., & Hurrell, R. F. (2007). Nutritional iron deficiency. *Lancet, 11*(370), 511-520.